NUCLEAR STRUCTURE

Rotational Bands in Odd-Odd ^{182}Re

M.F. Slaughter*, R.A. Warner+, T.L. Khoo≠, W.H. Kelly**, and Wm. C. McHarris

We have used in-beam γ-ray spectroscopic techniques to study the odd-odd deformed nucleus, ^{182}Re, resulting in probably the most complete analysis of an odd-odd nucleus yet reported. We used the ^{181}Ta(α,3nγ)^{182}Re, ^{182}W(p,nγ)^{182}Re, and ^{184}W(p,3nγ)^{182}Re reactions, with Ge γ-ray detectors in a variety of singles, coincidence, delayed coincidence, and angular distribution experiments. A complete paper has been submitted to Physical Review C,[1] and here we present a few highlights from this paper.

A singles γ-ray spectrum from the ^{181}Ta(α,3nγ)^{182}Re reaction is shown in Fig. 1, and some selected γ-γ coincidence gated spectra are shown in Fig. 2. Selected angular distributions are shown in Fig. 3, where they are fitted in the usual expansion in Legendre polynomials, with A_2 and A_4 coefficients being extracted.

The ^{182}Re level scheme we were able to construct from our data is shown in Fig. 4. Interestingly enough, only two rotational bands carry

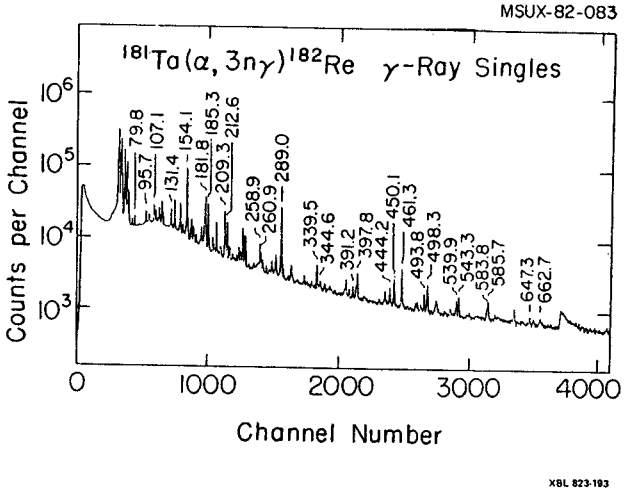

Fig. 1. Singles γ-ray spectrum from the ^{181}Ta(α,3nγ)^{182}Re reaction taken with a LEPS Ge(Li) detector. 61 γ-rays have been identified from ^{182}Re.

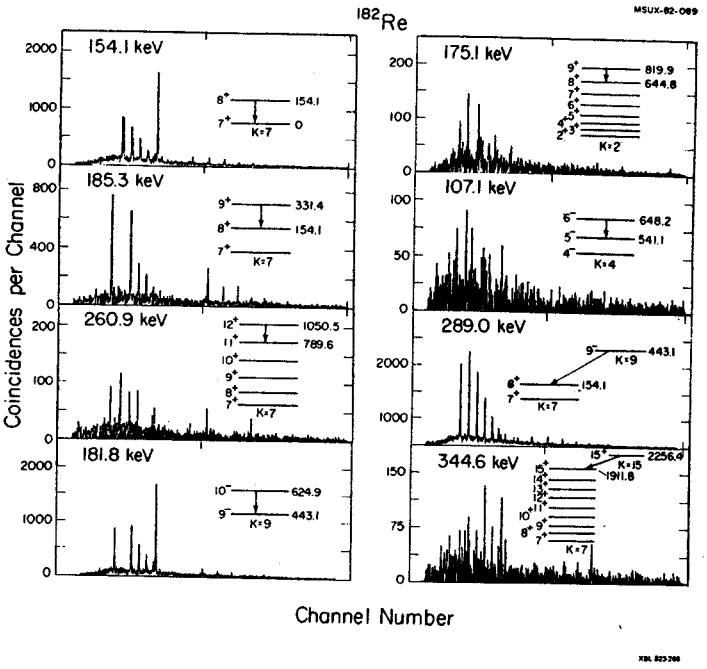

Fig. 2. Selected gated coincidence spectra from the ^{181}Ta(α,3nγ)^{182}Re reaction. They illustrate gates set on transitions within each of the four major rotational bands observed in ^{182}Re and also on two of the important interband transitions.

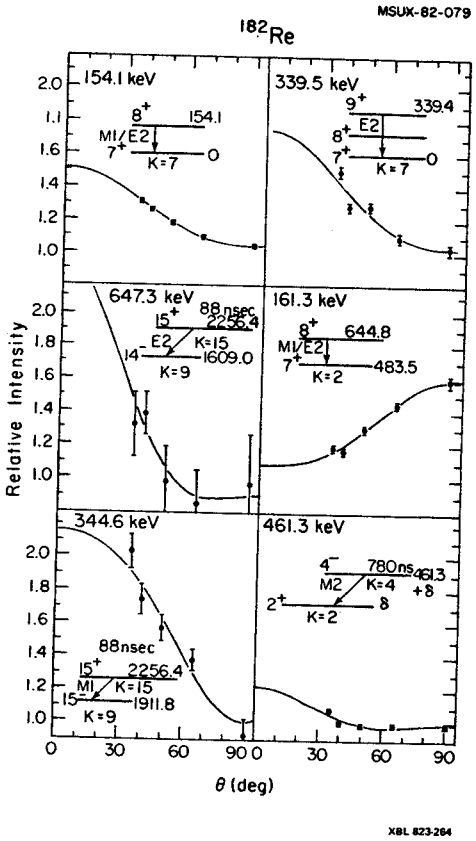

Fig. 3. Angular distributions for selected γ-rays from the ^{181}Ta(α,3nγ)^{182}Re reaction, showing examples of different multipolarities. The curves are least-squares fits to the data points.

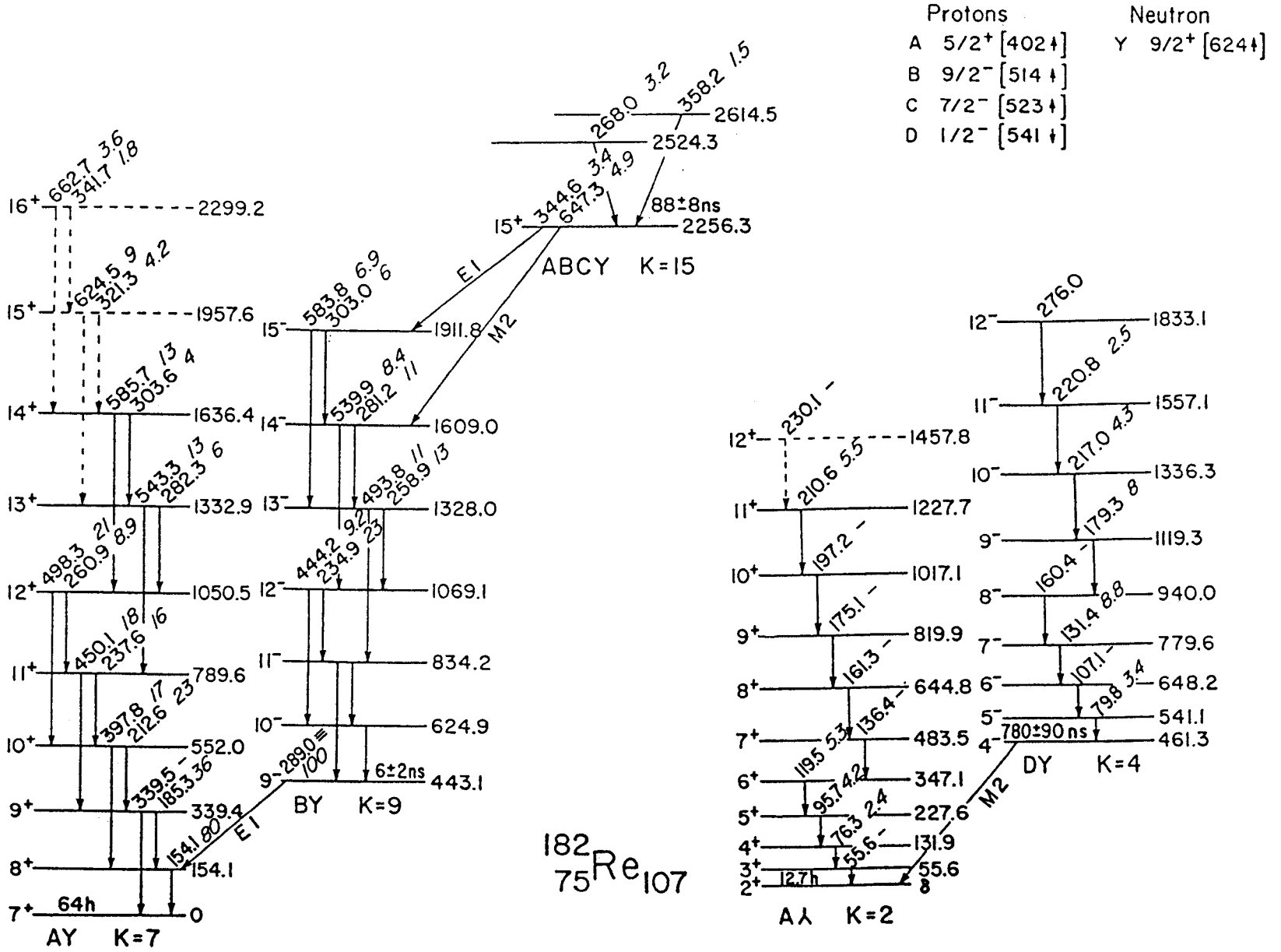

Fig. 4. ^{182}Re level scheme constructed from the present in-beam γ-ray data. All energies are given in keV, and γ-ray intensities (photon intensities not corrected for conversion) are normalized to the 289.0 keV transition. There is no observable isomeric transition between the 2^+ and 7^+ bands. The 7^+ band is presumed to be the ground state; consequently, energies of states in the 2^+ and 4^- bands must be increased by≈50 keV, the singlet-triplet coupling separation.

the bulk of the deexcitation, and only four are excited strongly enough to be characterized completely.[2] By means of delayed coincidence experiments we were also able to identify and place a $15^{(+)}$ multiparticle metastable state at 2256.3 keV.

We assigned configurations to the ^{182}Re bands by coupling the known low-lying states in the odd-mass neighboring nuclei. The only neutron state that appears to be involved is the $9/2^+[624\uparrow]$ Nilsson State. The 7^+ ground band of ^{182}Re is presumably the triplet coupling of the $5/2^+[402\uparrow]$ proton with this neutron state, the 2^+ band being the singlet coupling. The 9^- and 4^- bands then are the respective triplet couplings of the $9/2^-[514\uparrow]$ and $1/2^-[541\downarrow]$ protons with this same neutron state. The primary configuration of the four-particle state is less certain, but, if the deexciting γ-ray transitions are E1 and M2 (the E1 being very highly retarded as expected), it could well be the 15^+ configuration indicated (cf. Ref. 1). On the other hand, if the deexcitation transitions were M1 and E2, it could be a 15^- configuration, in which the $7/2^+[404\downarrow]$ proton is substituted for the $7/2^-$ $[523\uparrow]$ proton state.

All four major rotational bands are highly distorted by Coriolis coupling as expected: the $9/2^+[624\uparrow]$ neutron state originates from the $i_{13/2}$ state, and the $9/2^-[514\uparrow]$ and $1/2^-[541\downarrow]$ proton states originate from the $h_{11/2}$ and $h_{9/2}$ states, respectively - all of them have very large Coriolis matrix elements. Some of this distortion can be seen in Fig. 5, which is a standard "trumpet" plot. More significant, however, are the results illustrated in Fig. 6, a conventional plot designed to emphasize backbending. There is no apparent backbending, nor would we expect there to be, since we have not attained sufficiently large valves of $\vec{R}$ for it to occur. But the moments of inertia vary drastically from band to band; in particular, the difference between the 7^+ and 2^+ states should be noted, as these are presumably merely different couplings of the same (K-symmetrized) states. Evidently rotational alignment and decoupling are playing a large role.

For the 7^+ and 9^- bands we extracted values of δ and $|\, g_K - g_R \,|/Q_o$ both from our angular distribution results and from the M1/E2 branching ratios. These are given in Table I. In Table II we compare the calculated values of g_K with our experimental values - the agreement is quite good for our particular configuration assignments.

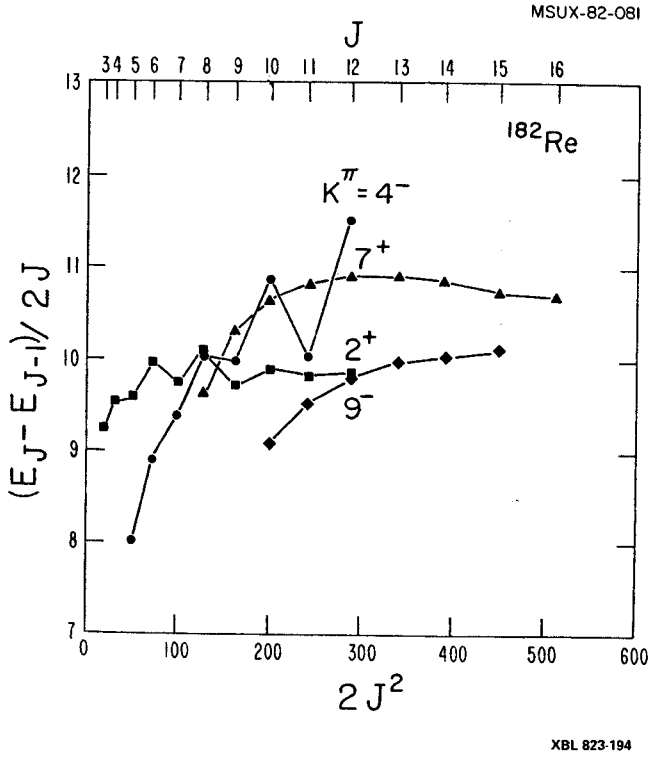

Fig. 5. Rotational spacings of lower-lying bands in ^{182}Re on a conventional "trumpet plot", demonstrating the large Coriolis distortions in these bands.

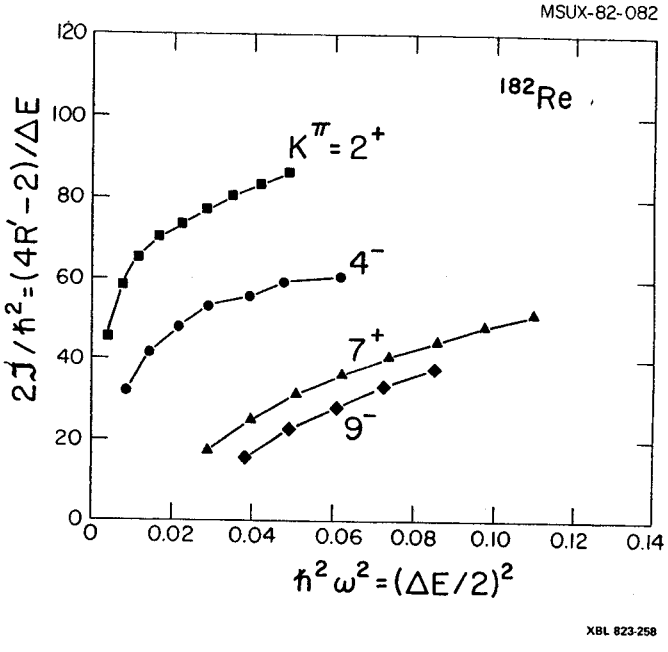

Fig. 6. A conventional "backbending plot", showing the large variation in moments of inertia of the various bands in ^{182}Re.

Table I. δ and $\left|\frac{g_K - g_R}{Q_o}\right|$ from Angular Distribution Results and Branching Ratios.

Cascade Transition (kev)	J_i	δ_{ad}	δ_{br}	$\left\|\frac{g_K - g_R}{Q_o}\right\|_{ad}$	$\left\|\frac{g_K - g_R}{Q_o}\right\|_{br}$
154.1	8^+	0.32 ± 0.03		0.056 ± 0.005	
185.3	9^+	0.39 ± 0.05	a	0.050 ± 0.006	
216.6	10^+	0.40 ± 0.06	0.42 ± 0.02	0.050 ± 0.007	0.048 ± 0.002
237.6	11^+	0.49 ± 0.07	0.42 ± 0.02	0.050 ± 0.006	0.048 ± 0.002
260.9	12^+	0.53 ± 0.11	a	0.038 ± 0.008	
282.3	13^+	0.50 ± 0.11	0.41 ± 0.02	0.041 ± 0.009	0.050 ± 0.003
303.6	14^+		0.47 ± 0.06		0.044 ± 0.006
			average =	0.046 ± 0.007	0.48 ± 0.002
181.8	10^-	0.23 ± 0.02		0.066 ± 0.005	
209.3	11^-	0.32 ± 0.03	0.33 ± 0.02	0.056 ± 0.005	0.055 ± 0.004
234.9	12^-	0.35 ± 0.05	0.34 ± 0.02	0.052 ± 0.007	0.054 ± 0.005
258.9	13^-	0.30 ± 0.07		0.062 ± 0.014	
281.2	14^-	0.42 ± 0.11	0.34 ± 0.02	0.071 ± 0.018	0.056 ± 0.004
303.0	15^-		0.36 ± 0.04		0.053 ± 0.005
			average =	0.061 ± 0.008	0.055 ± 0.001

[a]The quadrupole transition needed for the calculation of δ_{br} lies in an unresolved multiplet. Its intensity cannot be determined.

Table II. Calculated vs Experimental Values of g_K

Proton					
$5/2^+[402]$	$9/2^+[624]$	7	0.39	0.44	0.63
$5/2^+[402]$	$7/2^-[514]$	6	0.96	0.50	0.74
$9/2^-[514]$	$9/2^+[624]$	9	0.52	0.37	0.50
$7/2^+[404]$	$9/2^+[624]$	8	0.03	0.39	0.55
$5/2^+[402]$	$5/2^-[512]$	5	1.15	0.60	0.88
$5/2^+[402]$	$5/2^-[633]$	6	0.42	0.50	0.74

[a]Calculated from the asymptotic expression,

$$g_K = 1/K \quad (g_{sn}\Sigma_n + g_{\ell n}\Lambda_n) + (g_{sp}\Sigma_p \pm g_{\ell p}\Lambda_p) \ .$$

[b]Calculated from δ-ray branching ratios, assuming

$$Q_o = 6.4, \ g_R = 0.15, \text{ and } {}^{V}g_{s,eff} = 0.8 \ g_{s,free}.$$

A stylized representation of the four-particular states is shown in Fig. 7. The four uncoupled nucleons, although remaining in a prolate potential, provide a sort of "oblate girdle" about the nucleus. This could be a first step toward the so-called oblate-|| "effective rotations" predicted by Bohr and Mottelson.

In summary, odd-odd nuclei provide a rich potential for in-beam spectroscopic studies: 1) Their spectra are complex but not intractable. This comes about because of *"klokast"* states carrying the bulk of the deexcitation instead of its being spread out over a myriad of weakly-populated bands, as was previously feared. 2) Because of the large Coriolis couplings and distortions - and because of the potential for singlet and triplet couplings to have large Coriolis overlap through K=1/2 states - we have an added bonus for studying details of nuclear states. 3) Odd-odd nuclei have a head start over their neighbors in producing low-lying multiparticle states. These can be used to explore the possibilities of different, exotic couplings and collective motions. 4) There is no evidence of backbending, which is a (weak) argument against the pairing-collapse model and in favor of the decoupled pair model of backbending. However, because of the generally large values of Ω incountered in odd-odd nuclei, heavier projectiles are needed in order to excite large values of $\vec{R}$. This, is another illustration for the need of the newer generation of accelerators of very heavy ions.

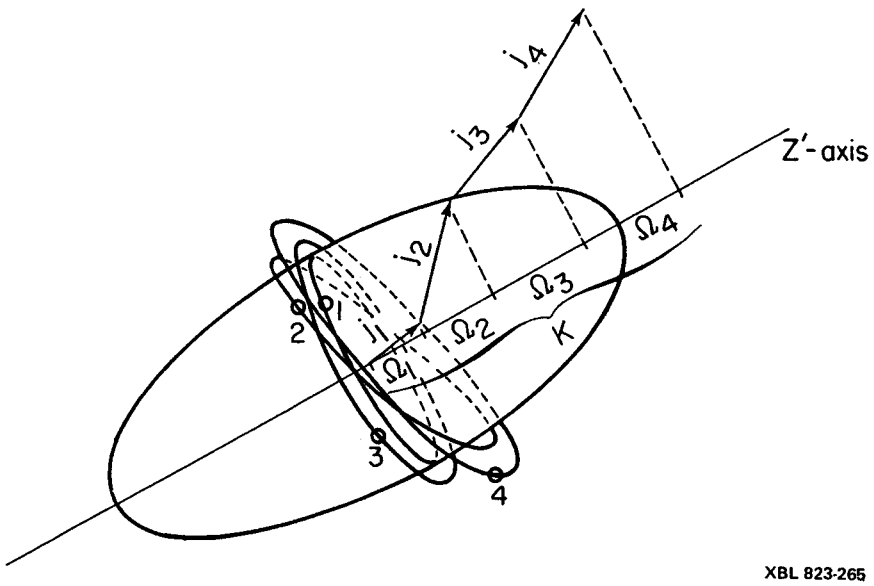

XBL 823-265

Fig. 7. Stylized sketch showing four high-Ω quasiparticles with their angular momenta uncoupled and aligned along the symmetry axis. Although still moving in a prolate potential, these four nucleons provide a first step toward an "effective" oblate rotation about the axis of symmetry.

---

* Present Address: Harvard Law School, Cambridge, Massachusetts 02138

+ Present Address: Battelle Pacific Northwest Laboratories, Richland, Washington 99352

≠ Present Address: Physics Division, Argonne National Laboratory, Argonne, IL 60439

** Present Address: Physics Department and Office of the Dean, Montana State University, Bozeman, Montana 59717

1. M.F. Slaughter, R.A. Warner, T.L. Khoo, W.H. Kelly, and Wm. C. McHarris, LBL-13968 and MSUCL-367, submitted to Phys. Rev. C (1982).

Decay Scheme of ^{254}Es

Z.M. Koenig, Wm. C. McHarris, I. Ahmad* and J. Milsted*

The odd-odd nucleus ^{254}Es decays by α emission with a 275.7-d half-life to its daughter ^{250}Bk, populating mostly excited levels which then decay by γ emission. It was first investigated by McHarris.[1] The source used in the present experiments were 10^3 times as hot as the source used originally. The experiments included α, γ, and e^- measurements in singles and various coincidence combinations, in which some 35 α and 45 γ-ray transitions were identified. Figures 1 and 2 are examples of α and γ-ray singles spectra, respectively.

All four low-lying rotational bands previously placed were confirmed and two new $K^\pi=6^+$ bands were placed, based on the triplet coupling of $\pi 7/2^+[633\uparrow]x\nu 5/2^+[622\uparrow]$ (at 355.3 keV) and $\pi 5/2^+[642\uparrow]x\nu 7/2^+[613\uparrow]$ (at 406.3 keV). Also, states were placed at 316.1 ($K^\pi = 5^+$) and 551.8 keV (K=8?).

On the basis of the present work and previous information, the decay scheme has been constructed; it is shown in Fig. 3. The levels have been grouped into rotational bands, and the experimental properties of these were compared with the predicted coupling of the odd-nucleon states found in neighboring odd-mass nuclei. The distortions of the bands in ^{250}Bk is explained by nuclear Coriolis interaction.

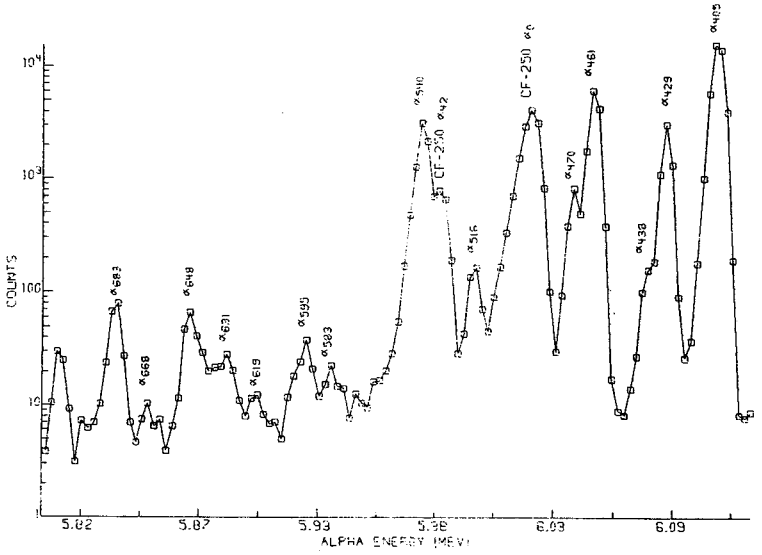

Fig. 1. Alpha-ray singles spectrum of ^{254}Es.

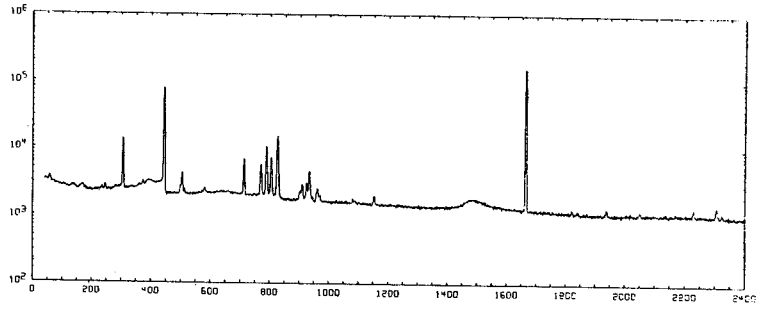

Fig. 2. Gamma-ray singles spectrum of ^{254}Es.

* Chemistry Division, Argonne National Lab., Argonne, IL.

1. Wm. C. McHarris, F.S. Stephens, F. Asaro, and I. Perlman, Phys. Rev. 144, 1031 (1966).

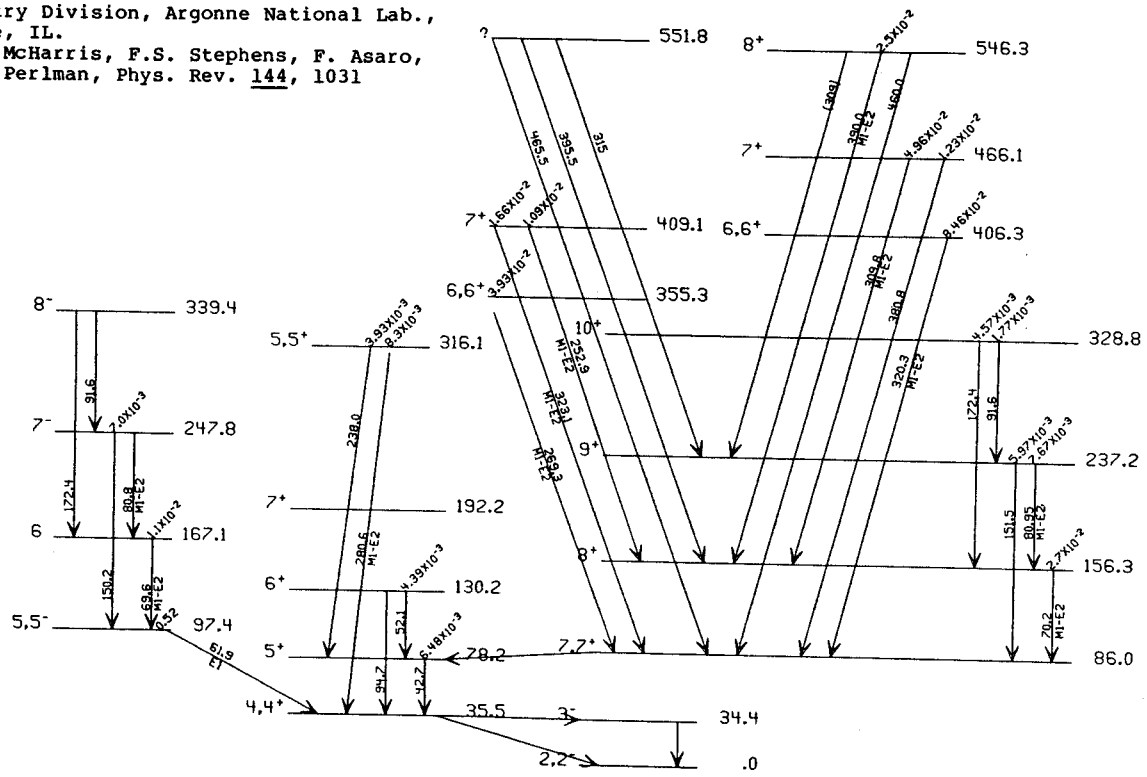

Fig. 3. Level diagram of ^{250}Bk.

Angular Distributions for ^{154}Sm, ^{166}Er $(\vec{p},p')$ Reaction at 134 MeV

R.M. Ronningen, N. Anantaraman, G.M. Crawley, B.M. Spicer*, G.G. Schute*, J.M.R. Wastell*, D.W. Devins**, and D.L. Friesel**

In last year's annual report[1] we presented motivational and experimental detail for a study of ^{154}Sm and ^{166}Er using the $(\vec{p},p')$ reaction at 134 MeV. During the past year all spectra were reduced to obtain cross sections and asymmetries for the 0^+, 2^+, 4^+, and 6^+ ground band states in both nuclei. We have now begun coupled channels analyses of these data.

Fig. 1 through 4 show data and coupled channels calculations for the cross sections and asymmetries. It is noteworthy that some magnitude and pronounced phase differences in both the cross section and particularly the asymmetry data are observed between the 6^+ states in ^{154}Sm in ^{166}Er. These may be due to differences in the deformation parameters β_4 and β_6. The calculations shown used a deformed version of the global spherical optical model potential of Nadasen et al.[2] The deformation parameters were obtained either from a previous study[3] in the case of ^{154}Sm, or from Coulomb excitation studies[4] in the case of ^{166}Er. (the deformation parameters from these studies were scaled for our potential by ratios of reduced radii of each optical model components so that the deformation lengths are nearly equal.)

Searches are now being carried out to determine values of standard optical model and deformation parameters which best fit the data.

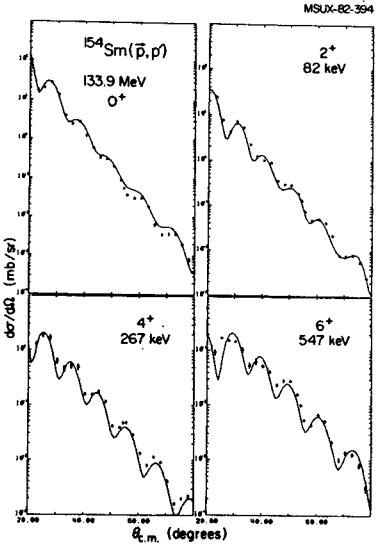

Fig. 1.

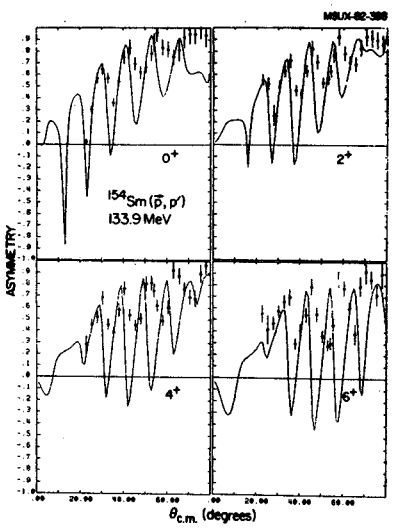

Fig. 2

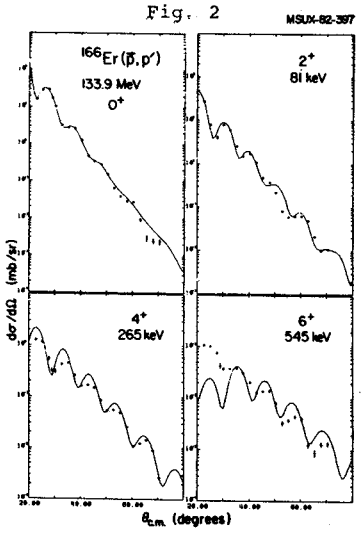

Fig. 3

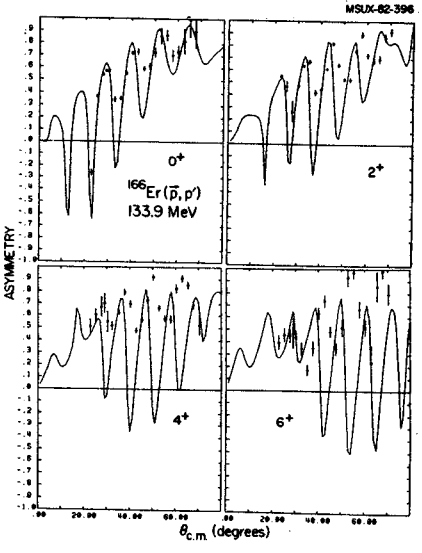

Fig. 4.

* University of Melbourne, Parkville, Victoria, Australia 3052
** Indiana University Cyclotron Facility, Bloomington, IN 47401
1. MSU Cyclotron Laboratory Annual Report 1980-81, pg. 47.
2. A. Nadasen et al., Phys. Rev. C 23, 1023 (1981).
3. MSU Cyclotron Laboratory Report 1978-79, pg. 25.
4. See R.M. Ronningen et al., Phys. Rev. C 16, 220 (1977).

Relation Between Spherical and Deformed Optical Model Potentials from ^{148,154}Sm (p,p') Reactions at 65 MeV

R.M. Ronningen, P.H. Debenham*, A. Gutermann**, D.L. Hendrie+, and A. Nadasen++

MSUX-82-398

It has been suggested[1] that the optical model potential can be expressed as a sum of two parts, one describing excitations of non-collective states and the second describing excitations of collective states. The latter can be treated explicitly given a suitable model for collective excitations and current techniques for solving coupled-channels equations. It in principle contains information on the nuclear shape. On the other hand, the former is inherently independent of shape and should vary smoothly for a wide range of nuclei. Thus, for example, to describe the excitations of rotational states in a deformed nucleus one should need only to introduce deformation parameters into the optical potential for a neighboring spherical nucleus.

This approach has been tested[1] for (α,α') reactions at 50 MeV on ^{148,154}Sm. We report here tests for the (p,p') reaction at 65 MeV on the same nuclei using data taken at the University of Maryland Cyclotron Facility.

Data on ^{148}Sm were analyzed first using standard optical model and DWBA codes. Then, the resulting optical model potential parameter values were refined using the code[2] ECIS, in which the elastic and first excited 2^+ state were coupled within the framework of the vibrational model. The results are shown in Fig. 1 and the potential parameters are given in Table 1.

The nucleus ^{154}Sm was treated as a rigid rotor in coupled channels calculations using ECIS. The optical model parameters are in Table 1 as well as the deformation parameters β_2 and β_4. In the calculation shown in Fig. 2, β_2 and β_4 were "βR"-scaled from those used in the Coulomb potential, which reproduce the E2 and E4 moments measured using Coulomb excitation.

It is obvious from comparing the data and calculations that only a minor adjustment of the "spherical" part of the optical model potential for ^{154}Sm will provide an optimal fit to the elastic scattering data. This is presently being done as well as searching for best values for β_2 and β_4. Also, we are investigating the influence of the β_6 deformation parameters. The multipole moments of the optical model potential will be extracted to obtain shape information.

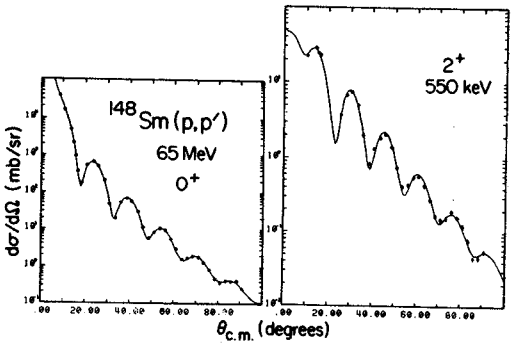

Table 1. Spherical Optical Model Parameters for ^{148}Sm and Deformation Parameters for ^{154}Sm.

OM Parameters[a] for ^{148}Sm		Deformation parameters for ^{154}Sm "βR" scaled	
V	35.99	β_{2r}	0.243
W	4.72	β_{2i}	0.218
W_d	2.89	β_{2so}	0.246
V_{so}	5.01	β_{2coul}	0.274
W_{so}	-0.24	β_{4r}	0.091
a_r	0.701	β_{4i}	0.082
a_i	0.678	β_{4so}	0.093
a_{so}	0.825	β_{4coul}	0.103
a_{coul}	0.600		
r_r	1.240		
r_i	1.383		
r_{so}	1.225		
r_{coul}	1.100		

a. The unit for well depth is MeV, for diffuseness and radius, fm.

MSUX-82-395

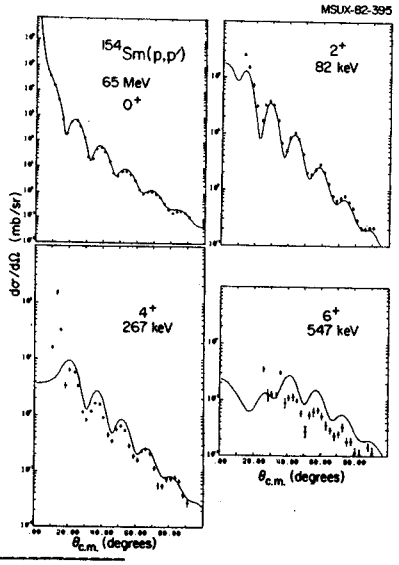

* University of Maryland. Present address: National Bureau of Standards, B-102, Bldg. 245, Washington, D.C. 20234.
** University of Maryland. Present address: Department of Physics, Tel Aviv University, Israel.
+ University of Maryland. Present address: Department of Energy, ER-23/GTN, Washington, D.C. 20545.
++ University of Maryland.

1. N.K. Glendenning, D.L. Hendrie, and O.N. Jarvis, Phys. Lett. 26B, 131 (1968).
2. J. Raynal, unpublished.

Excitation of ℓ=0, Spin-Flip Transitions in (p,p') Reactions at 200 MeV

N. Anantaraman, G.M. Crawley, J. Duffy, A. Galonsky, C. Djalali*, J.-C. Jourdain*, N. Marty*, M. Morlet*, and A. Willis

In the (p,p') reaction at 200 MeV, ℓ=0, spin-flip (M1) transitions are enhanced above most other transitions when observed at small angles. With the synchrocyclotron and magnetic spectrometer at Orsay we have been able to make such observations down to 3° for many targets[1,2] and to 2° for ^{48}Ca. To date we have completed measurements on 19 targets, and we have some data on six other targets. The target mass number ranges from 40 to 140.

A set of spectra obtained at 4° with some nickel targets is shown in Fig. 1. The broad, structured peak found around 9 MeV in each of these spectra is representative of the small-angle spectra of all the heavier targets. By comparison of the angular distribution of the broad peak with DWBA calculations, it is established that the peak consists of a concentration of ℓ=0 strength. The spin-flip dominance of the transition is a property of the effective nucleon-nucleon interaction[3] at 200 MeV. The nuclear shell-model transition induced is between spin-orbit partners, mainly $f_{7/2} \rightarrow f_{5/2}$ in the nickel targets.

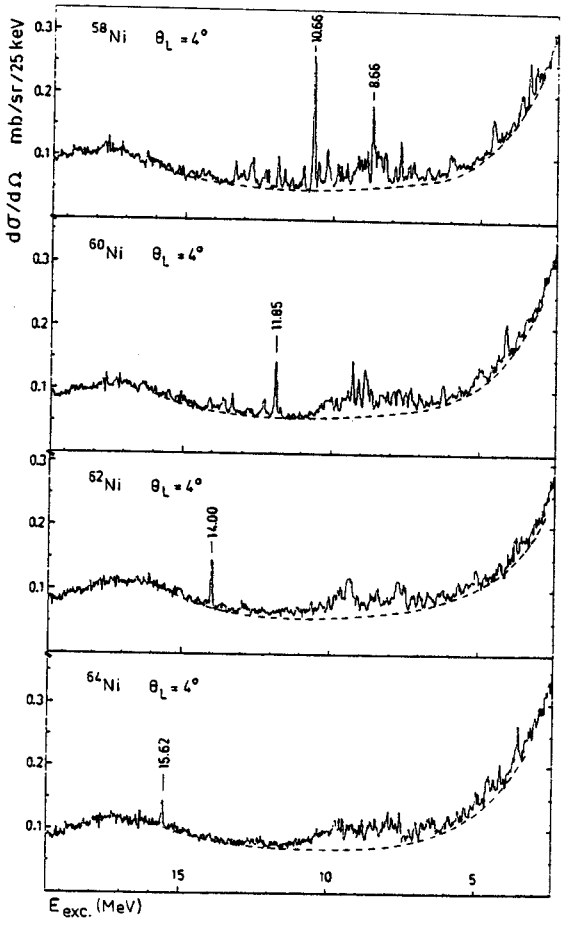

Fig. 1.

Spin-flip dominance is even more specifically determined by the N-N interaction in that the isovector part, $V_{\sigma\tau}$, is considerably greater than the isoscalar part, V_{σ}. The isovector part can induce transitions from states of isospin T_o to states having either T_o or T_o+1 if both neutrons and protons in the target are excited (and if $T_o \neq 0$). The nickel isotopes constitute such targets, and the sharp peaks at 10.66, 11.85, 14.00, and 15.62 MeV in Fig. 1 are presumably T_o+1 states in ^{58,60,62,64}Ni, respectively. As expected, their isospin splitting from the broad T_o peak around 9 MeV increases with T_o and is in rough agreement with the formula

$$E_{T_o+1} - E_{T_o} = \frac{V_1}{A} (T_o+1) \text{ for } V_1 \simeq 80 \text{ MeV}.$$

Sharp peaks at high excitation energy imply an inhibition against decay. For the four sharp peaks cited above, the Coulomb-centrifugal barrier produces a charged-particle decay width much smaller than the instrumental width of ≈ 70 keV. Inhibition against neutron decay can be obtained only if $T > T_o$ (presumably T_o+1) so that isospin could not then be conserved. Corroborating evidence of the T_o+1 assignment has now been obtained in a (p,n) experiment on the same target nuclei, and a report on that work (by Anantaraman et al.) appears elsewhere in this progress report.

Spectra from some of the other targets are shown in Figs. 2 and 3. Each of these targets has 28 neutrons, i.e., a full $f_{7/2}$ shell and an empty $f_{5/2}$ shell. The ^{54}Fe and ^{50}Ti targets have, in addition, some protons in the $f_{7/2}$ shell, whereas the ^{48}Ca $f_{7/2}$ shell is void of protons. In accordance with the earlier discussion we would, therefore, expect spectra at a small angle, such as 4°, the angle for Fig. 2, to show excitation of 1^+ states having isospin T_o and others having T_o+1 in ^{54}Fe and in ^{50}Ti, but only T_o in ^{48}Ca. The occurrence of a single line in the ^{48}Ca spectrum and a multiplicity of lines in ^{50}Ti and ^{54}Fe is consistent with this expectation, but identification of T_o and T_o+1 lines in the latter two spectra is not possible.

Detailed investigation of ^{48}Ca should be fruitful because of the simplicity of its shell-model wave function. Indeed, in no other target have we seen such an extreme concentration of ℓ=0, spin-flip strength. As shown in Fig. 3, this concentration allows a beautiful demonstration of the ℓ=0 selectivity at small angles.

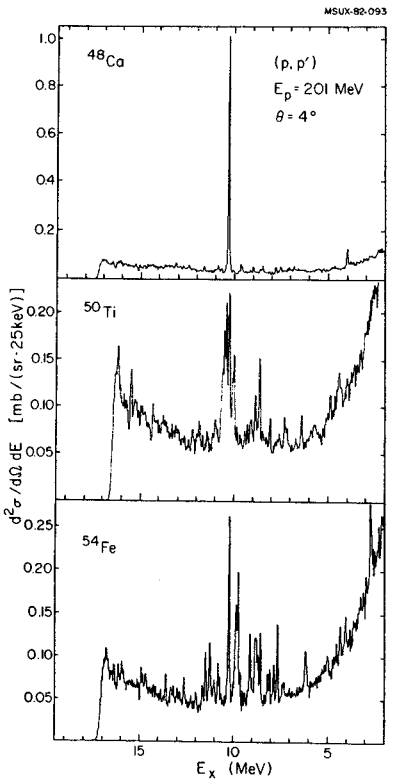

Fig. 2.

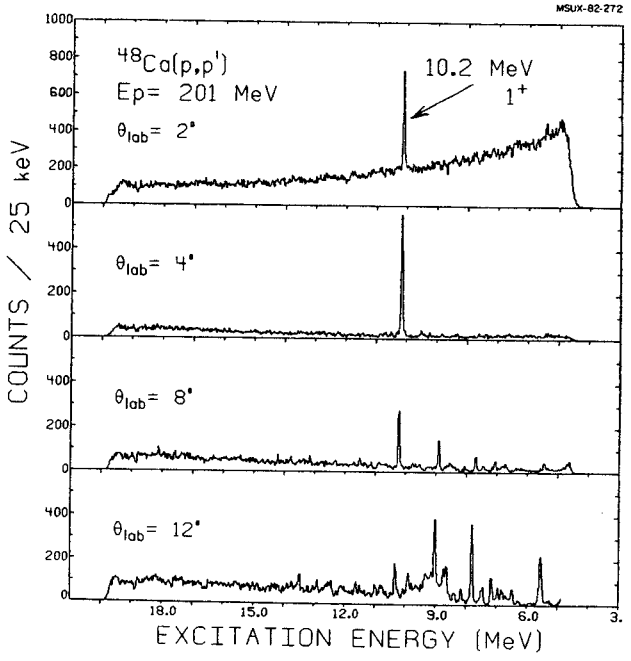

Fig. 3.

When both the theoretical and experimental structures are so simple one would feel justified in taking seriously significant discrepancies. Under less favorable conditions, i.e., for nuclei from ^{58}Ni to ^{140}Ce, the absolute value of the cross section has been overpredicted[1,2] by standard nuclear physics calculations. A similar discrepancy has been found for (p,n) cross sections to anti analogues of the type of giant M1 states discussed here. A popular remedy that has been proposed[4] is to include in the usual neutron-proton structure of nuclei the J=3/2, T=3/2 Δ resonance. Then, in addition to producing NN^{-1} pairs, the $V_{\sigma\tau}$ interaction can produce ΔN^{-1} pairs. Since the mass of the Δ requires such excitations to have ~300 MeV of energy, the NN^{-1} excitations observed in experiments such as ours should account for only part of the $V_{\sigma\tau}$ excitation. To test this fundamental idea it is important to use cases which are as clear as possible. ^{48}Ca(p,p') is one of these. Two comparisons with the data are shown in Fig. 4. One is the widely-used DWBA70 of J. Raynal and R. Schaeffer with the interaction[3] of Love and Franey. The other, RESEDA, the work of A. Willis[5], works directly from the latest nucleon-nucleon phase shifts[6] and should be equally valid. Although neither calculation fits the data at the larger angles, both give acceptable fits out to 10°. However, to better compare the shapes of theory and experiment, the absolute values of the calculated curves have been altered to match experiment at 5°. In fact, the ratio of experiment to theory is 0.23 for both DWBA70 and RESEDA. It seems clear that there is room for more experimental cross section, perhaps by ΔN^{-1} excitations.

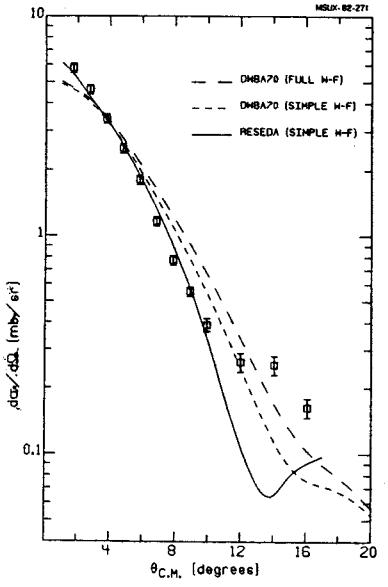

Fig. 4.

* Institut de Physique Nucléaire, Orsay, France.

1. G.M. Crawley, N. Anantaraman, A. Galonsky, C. Djalali, N. Marty, M. Morlet, A. Willis, J.-C. Jourdain, and P. Kitching, Phys. Rev. C26, 87 (1982).
2. C. Djalali, N. Marty, M. Morlet, A. Willis, J.-C. Jourdain, N. Anantaraman, G.M. Crawley, A. Galonsky, and P. Kitching, Nucl. Phys. A388,1(1982).
3. W.G. Love and M.A. Franey, Phys. Rev. C24, 1073 (1981).
4. E. Oset and M. Rho, Phys. Rev. Lett. 42, 47 (1979) and M. Ericson, A. Figureau, and C.T. Thevenet, Phys. Lett. 95B, 349 (1980).
5. A. Willis, Ph.D. thesis, Orsay 1968 (unpublished) and C. Djalali, N. Marty, M. Morlet, and A. Willis, Nucl. Phys. A380, 42 (1982).
6. R.A. Arndt, R.H. Hackman, and L.O. Roper, Phys. Rev. C 15, 1002 (1977).

Measurements of Gamow-Teller Strength for Double-Beta Decaying Nuclei via the (p,n) Reaction at 134 MeV

Sam M. Austin, R. Madey*, J.W. Watson*, B.D. Anderson*, A. Baldwin*, B.S. Flanders*, C. Lebo*, and C.C. Foster**.

Double β decay (denoted ββ decay)[1] can occur in two modes:

$$(Z,A)\rightarrow(Z+2,A) + e_1^- + e_2^- + \bar{\nu}_1 + \bar{\nu}_2 \quad (2\nu)$$

$$(Z,A)\rightarrow(Z+2,A) + e_1^- + e_2^- \quad (0\nu)$$

The first of these modes can be thought of as a second order process, a sequence of two normal β decays passing through (virtual) intermediate states of the nucleus (Z+1,A). The second is of great fundamental interest since it does not conserve lepton number.

Recently there has been a renewed interest in these decays because limits on the (0ν) branch for ^{82}Se and ^{76}Ge decay have been used to place limits on the masses of Majorana neutrinos[2] and because the first direct electron counting experiment[3] has been performed for $^{82}Se\rightarrow^{82}Kr+2e^-+2\bar{\nu}$, yielding a lifetime of $1.0 \pm 0.4 \times 10^{19}$ years. This is about a factor of thirty shorter than the lifetime obtained by geochemical methods. A detailed model calculation of the (2ν) lifetime has been performed by Haxton, Stephenson and Strottman (HSS)[2] and is in good agreement with the direct counting result but not with the geochemical results for ^{82}Se or ^{76}Ge. Other analyses based on the experimental ratio of the lifetimes for ^{128}Te and ^{130}Te have argued that the non-lepton conserving 0ν process has been observed. This argument involves only the assumption[4] that the ββ matrix elements for ^{128}Te and ^{130}Te are the same. Theoretical shell model calculations[5] bear out this assumption but also greatly overestimate the strength of the transition, weakening the conclusion about the ratio.

In an attempt to provide constraints on the calculations we have used the neutron time-of-flight system at the Indiana University Cyclotron Facility to obtain (p,n) spectra at 0°, 4° and 8° for ^{76}Ge, ^{82}Se and ^{128,130}Te. The flight path was 85 m and overall time resolution was 750 psec, corresponding to an energy resolution of 360 keV. The L=0 strength at 0° (low q) is closely proportional to the Gamow-Teller (GT) strength to the (virtual) intermediate states of the ββ process. Strength is observed to the giant GT resonance region and to narrow low lying structures populated with $\sim 10^{-2}$ the strength of the giant resonance. The spectrum for ^{82}Se is shown in Fig. 1.

The results for ^{128,130}Te are simplest to interpret, since the ββ decay analysis assumes only that the matrix elements are the same.

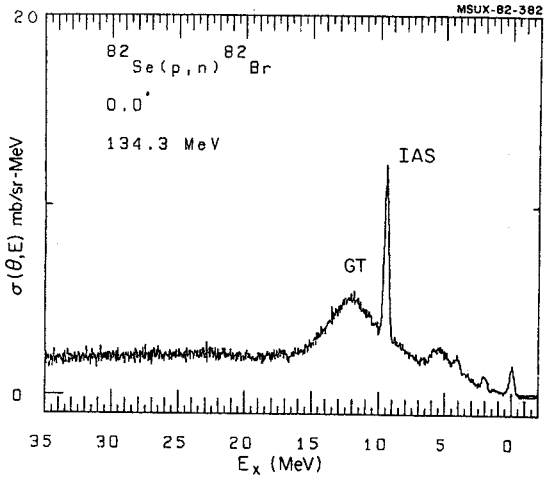

Fig. 1. Spectrum for ^{82}Se (p,n) at 0° and E_p=134 MeV.

Since the Fermi-like (L=0,S=0) transition to the isobaric analog state (IAS) is proportional to (N-Z) for the target, an estimate of the differences in the GT strengths, independent of many systematic errors, can be obtained by normalizing the spectra so the IAS yield is proportional to N-Z. This has been done for the spectrum shown in Fig. 2 where we plot the quantity

$$\frac{Y(^{130}Te)-Y(^{128}Te)}{Y(^{130}Te)}$$

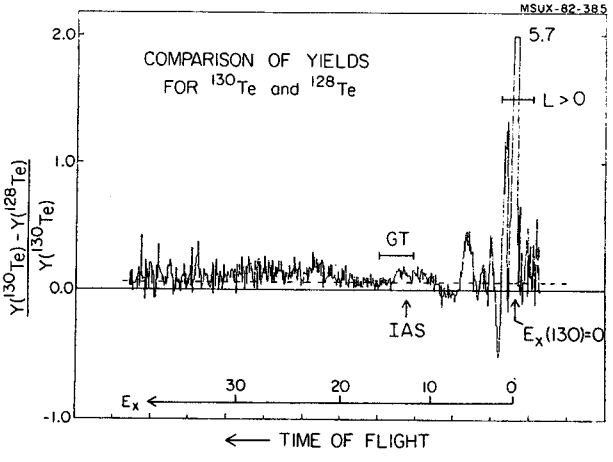

Fig. 2. Normalized fractional difference in yields for ^{128}Te and ^{130}Te at E_p=134 MeV. The positions of the IAS and GT giant resonances are indicated.

Here the Y's are the yields for the noted nucleus, normalized as discussed above. To the extent that only L=0 GT strength is observed at 0°, a good approximation in the neighborhood of the giant Gamow-Teller resonance, the plotted ratio

is also the fractional difference of the allowed (L=0) GT strength for ^{128}Te and ^{130}Te. We see that this difference is less than 15% in the neighborhood of the giant GT resonance. (Since summed Gamow-Teller strength is also porportional to N-Z we might expect a ratio of 13/12). At low excitation the GT strengths differ markedly but a rather small portion of the total strength is involved and moreover, this strength is mostly L>0 and does not contribute to the $\beta\beta$ process.

---

* Kent State University
** Indiana University Cyclotron Facility

1. D. Bryman and C. Picciotto, Rev. Mod. Phys. 50, 11 (1978).
2. W.C. Haxton, G.J. Stephenson and D. Strottman, Phys. Rev. Lett. 47, 153 (1981).
3. M.K. Moe and D.D. Lowenthal, Phys. Rev. C22, 2186 (1980).
4. B. Pontecorvo, Phys. Lett. 26B, 630 (1968).
5. W.C. Haxton, et al, preprint.

Gamow-Teller Strength in the ^{26}Mg (p,n) ^{26}Al Reaction at 134 MeV

S.M. Austin, A. Galonsky, B.H. Wildenthal, B.D. Anderson*, A.R. Baldwin*, C. Lebo*, R. Madey*, J.W. Watson*, B.S. Flanders**, and C.C. Foster**

Neutron spectra at several angles near 0° have been measured for the titled reaction with protons from the Indiana University Cyclotron and with the Kent State University detection system. Through the spinflip-isospinflip interaction such spectra should show enhanced excitation of 1^+ states. A 0° spectrum is shown in the Fig. Except for the 0^+ isobaric analog of the target ground state, all of the more prominent structure very likely belongs to 1^+ states.

Because the (p,n) interaction is necessarily isovector and the target has isospin T_o=1, the states of the final nucleus (with T_z=0) have T=0, 1, and 2. Known T=0, 1^+ states at low excitation are labelled 1^+ in the Fig. The strength observed between about 8.5 and 13 MeV should be the T=1 isobaric analog of 1^+ strength known from backward-angle (e,e') experiments.[1] Each of the four peaks with an arrow above it has an ℓ=0 angular distribution and, presumably, corresponds to 1^+ strength. Indeed, the strongest of these peaks has an excitation energy, 13.6 MeV, that does correspond, via Coulomb displacement energy, with a strong M1 excitation in ^{26}Mg (e,e').[2] Furthermore, via two Coulomb displacements, 13.6 MeV in ^{26}Al corresponds to 0.1 MeV in ^{26}Na, where there is a state[3] of undetermined spin and parity. Hence, the peak at 13.6 MeV in the (p,n) spectrum may correspond to a 1^+ state with T=2. The three other 1^+ peak, because of their high excitation energies, may also represent T=2 strength.

It is intended that the spectroscopic information obtained here on Gamow-Teller strength will, in combination with B(M1) values, be interpreted in terms of a global model of the s-d shell.

---

* Kent State University
** Indiana University

1. L.W. Fagg, Rev. Mod. Phys. 47, 683 (1975).
2. W.L. Bendel et al., Phys. Rev. 173, 1103 (1968).
3. E.R. Flynn and J.D. Garrett, Phys. Rev. C 9, 210 (1974).

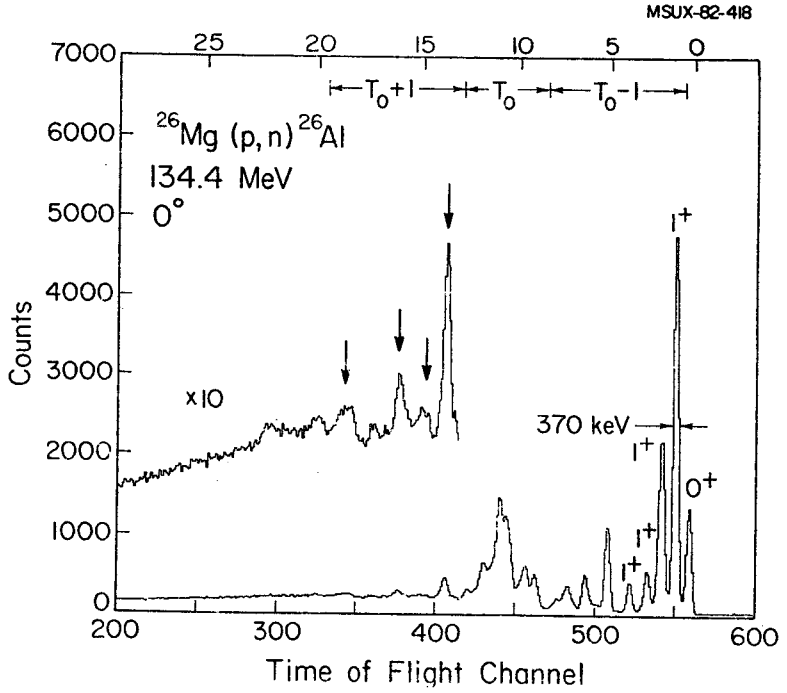

Study of Higher Isospin Components of Gamow-Teller Strength in Ni(p,n) Reactions

N. Anantaraman, S.M. Austin, G.M. Crawley, A. Galonsky, H. Toki, B.D. Anderson*, A.R. Baldwin*, C. Lebo*, R. Madey*, J.W. Watson*, and C.C. Foster**

The observation,[1] in high-energy inelastic proton scattering, of peaks that are believed to be the T_o and (T_o+1) components of the Ml resonance in the even Ni isotopes is reported elsewhere in this volume. Here T_o is the isospin of the target ground state. Motivated by this observation, we undertook a study of the (p,n) reaction on the even Ni isotopes to excite the analogues of these states, as well as the dominant (T_o-1) 1^+ component. The hope was that the observed strengths to the various 1^+ states in the (p,p') and (p,n) reactions would help in refining and testing a detailed model of the structure of these states.

It has become very clear in the last few years that the (p,n) reaction at high energies (E>100 MeV) and forward angles selectively excites the Gamow-Teller (1^+) states in nuclei, with the main strength occurring in the giant (T_o-1) component.[2] The T_o and (T_o+1) components are expected to be populated more weakly in general, partly as a result of isospin coupling geometry. There exist a few (p,n) studies in which the weak T_o component has been separated from the (T_o-1) part, but no observation of the (T_o+1) part has been reported in medium-mass or heavy nuclei.

The measurements were performed at the neutron time-of-flight setup of the Indiana University Cyclotron Facility using a 134 MeV proton beam. A flight path of 86 meters and target thicknesses ranging between 36 and 50 mg/cm^2 combined to give a resolution of about 400 keV. The isotopic enrichment was above 99% for ^{58,60,62}Ni, and was 96.5% for ^{64}Ni. The neutrons were detected in three mean-timed plastic scintillators with a total size of 60" x 40" x 4". Spectra were measured in 4^o steps from 0^o to 12^o.

The 0^o (p,n) spectra for the four targets are shown in Fig. 1. The ground-state isobaric analogue state (IAS) occurs at excitations of 0.2, 2.5, 4.6 and 6.8 MeV, respectively, in ^{58,60,62,64}Cu. By adding to the IAS energies the T_o and (T_o+1) excitation energies observed in (p,p'), the positions of these isospin components in the (p,n) spectra can be predicted. The comparison between the predicted and observed positions is shown in Table I. Based on this comparison, we tentatively make the isospin assignments indicated in Table I to some of the (p,n) peaks. The comparison works better for the (T_o+1) levels than for the T_o levels. This is not surprising, since in (p,p') the T_o peak is broad (with a great deal of fine structure) while the (T_o+1) peak is sharp; this makes the determination of the centroid energy less certain for the former. The (T_o+1) level is not observed in ^{64}Cu, probably because it is too weak.

The remaining broad structures in the spectra, at excitations above 5.5 MeV, are given the isospin assignment (T_o-1). We emphasize that such division of the observed peaks into different isospin components is open to question, and that it is possible that there is an overlapping of Gamow-Teller strength for the different isospin components. However, inspection of the spectra indicates that the (T_o+1) strengths in ^{60,62}Cu and the T_o strengths in ^{62,64}Cu can be determined with reasonable precision. Extraction of yields, with the backgrounds shown by the solid lines in Fig. 1, is under way.

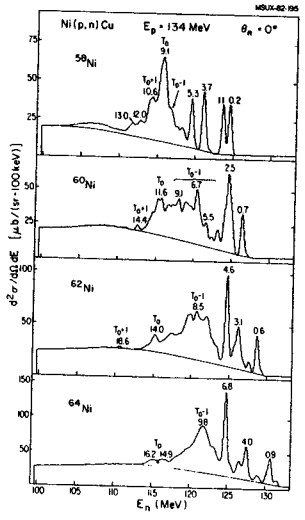

Fig. 1. Spectra of neutrons from $^{58/60/62/64}$Ni (p,n) reactions at 0^o.

Table I. Expected and observed energies of T_o and (T_o+1) 1^+ states in Cu isotopes.

Nucleus	Energy in Parent Nucleus* (MeV) T_o	T_o+1	IAS Energy (MeV)	Expected Energy (MeV) T_o	T_o+1	Observed Energy (MeV) T_o	T_o+1
^{58}Cu	8.5	10.7	0.2	8.7	10.9	9.1	10.7
^{60}Cu	8.9	11.9	2.5	11.4	14.4	11.6	14.4
^{62}Cu	8.8	14.0	4.6	13.4	18.6	14.0	18.6
^{64}Cu	8.9	15.6	6.8	15.7	22.4	14.9, 16.2	----

* From the (p,p') data of reference 1.

* Department of Physics, Kent State University, Kent, Ohio 44242
** Indiana University Cyclotron Facility, Bloomington, Indiana 47405

1. C. Djalali et al., Nucl. Phys. A 388 (1982)1
2. C.D. Goodman, Nucl. Phys. A374 (1982) 241.

Highly Excited Hole Strength Observed in the $^{90}Zr(\vec{p},d)\ ^{89}Zr$ Reaction

J. Kasagi, G.M. Crawley, E. Kashy, J. Duffy, D. Friesel*, S. Gales** and E. Gerlic**

Deeply bound hole states in medium and heavy nuclei observed in one nucleon pickup reactions are characterized by giant resonance-like broad bumps at an excitation energy of several MeV.[1] The single hole strength is considered to be fragmented by the coupling with the collective phonon-particle states[2] or with the core polarized states.[3] Additional spreading results from the small mixing of these states with many close-lying states. Therefore, the observation of the shape of the deep hole states gives important information about the mechanism of the fragmentation of highly excited states in nuclei.

So far, $1g_{9/2}$ neutron hole states has been extensively studied for the Sn isotopes[4] and $1g_{9/2}$ proton hole states has been studied for the Pm isotopes.[5] The results suggested that there exist differences of the spreading mechanism between the neutron and proton hole states.[5] The $1f_{7/2}$ shell is a more favorable case to study the strength distribution because of its isolation from both valence and inner shells. Recently, the broad bump observed at Ex ≈ 5 MeV in the $^{90}Zr(d,^3He)^{89}Y$ reaction has been unambiguously assigned to be $1f_{7/2}$ hole states by analyzing power measurements.[6] The $1f_{7/2}$ bump is well separated from the low-lying states and shows a rather symmetric shape with a few peaks around 5 MeV. On the other hand, the $1f_{7/2}$ neutron hole strength, observed in the $^{90}Zr(^3He,\alpha)^{89}Zr$ reaction recently reported by Duhamel et al.,[7] was distributed quite differently from the proton hole case. The reported $1f_{7/2}$ neutron hole strength is distributed rather continuously from $E_x \approx 3.5$ MeV to $E_x \approx 20$ MeV with several peaks around 5 MeV. However in the latter experiments, unique spin assignments have not been made and therefore the possibility of the existence of $1f_{5/2}$ hole states at $E_x \gtrsim 3.5$ MeV is not excluded.

We report here the study of the $^{90}Zr(p,d)^{89}Zr$ at 90 MeV, and the results show that the broad structure between $E_x \approx 3.5$ MeV and $E_x \approx 7.0$ MeV are not $if_{7/2}$ hole states but mainly $1f_{5/2}$ hole states. As reported in ref. 8, unambiguous spin assignments were possible by measuring the analyzing power in the $(\vec{p},d)$ reaction.

The experiment was performed using a 90 MeV polarized proton beam from the Indiana University Cyclotron. The experimental details are given in ref. 8.

An energy spectrum at 20° is shown in Fig. 1. Because of the angular momentum matching the ground state ($9/2^+$) and 1.46-MeV state ($5/2^-$) are seen prominently among the low-lying states.

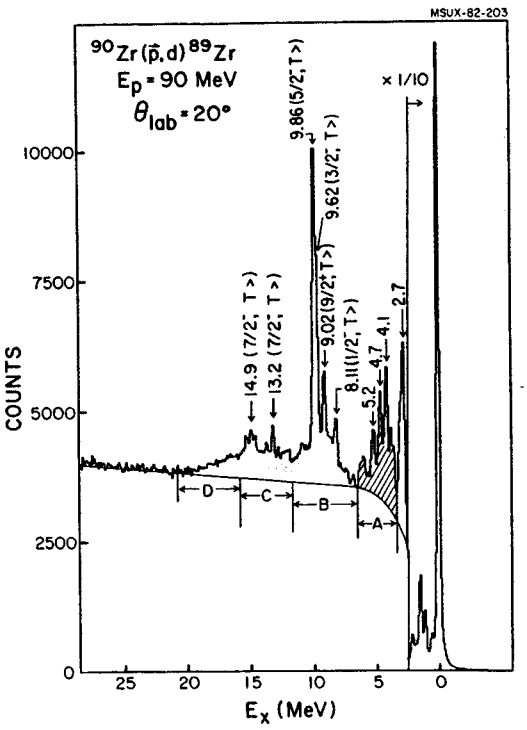

Fig. 1.

All these structures are proposed to be $J = 7/2^-$ in ref. 7 and 9 based on the angular distributions and the S-factor arguments except the region near 20 MeV where some 1d strength has been reported.[7] The analyzing power measurements were used to determine the spin of these broad structure. We normalized in such a way that the total S-factor of the $1g_{9/2}$ orbit is set equal to the sum-rule limit (10).

The characteristic features of the high-lying hole states of ^{89}Zr observed in the (p,d) reaction can be summarized as follows. The gross structure lying between 3.3 MeV and 22 MeV can be separated by the minimum at about 7.0 MeV. The structure between 3.3 and 7.0 MeV which was proposed to be $(1f_{7/2})^{-1}$ has been shown to be mainly from $1f_{5/2}$ pickup. The $(1f_{7/2})^{-1}$ strength in this excitation region is found in the 4.1 MeV and 5.2 MeV peaks, which have only 8% of the total observed $(1f_{7/2})^{-1}$ strength. On the other hand, the strength of the $(1f_{5/2})^{-1}$ found in this region is about 1/4 of the total $(1f_{5/2})^{-1}$ strength observed. About half of the total $(1f_{5/2})^{-1}$ strength is concentrated in the 1.45 MeV peak and this strength is terminated by about 7 MeV.

Beyond 7 MeV, almost all the $(1f_{7/2})^{-1}$ strength is found in the gross structure which continues

up to about 20 MeV. Therefore, the broad structure of $T_>$ $(1f_{7/2})^{-1}$ states can be expected to be between 12 and 19 MeV. However there is no clear separation between $T_>$, and $T_<$ states. The $T_<$ states may be distributed very broadly between 7.0 and 15 MeV, and in the 4.1 and 5.2 MeV peaks. The analysis of these results is continuing.

---

* IUCF, Bloomington, IN.
** IPN, Orsay, France.

1. M. Sakai and K.I. Kubo, Nucl. Phys. A185 (1972) 217.
2. T. Koeling and F. Iachello, Nucl. Phys. A295 (1978) 45.
3. M. Nomura, Prog. Theor. Phys. 55 (1976) 622.
4. E. Gerlic et al., Phys. Lett. 57B (1975) 338, Phys. Rev. C21 (1980) 126; M. Sekiguichi et al., Nucl. Phys. A278 (1977) 231; M. Tanaka et al., Phys. Lett. 78B (1978) 221; R.H. Siemssen et al., Phys. Lett. 103B (1981) 323.
5. P. Doll et al., Phys. Lett. 82B (1979) 357.
6. A. Stuirbrink et al., Z. Phys. A297 (1980) 307.
7. G. Dugamel et al., J. Phys. G7 (1981) 1415.
8. G.M. Crawley et al., Phys. Rev. C23 (1981) 1818.
9. S. Gales et al., Nucl. Phys. A288 (1977) 221.

Experimental Evidence for Giant Multipole Strength up to 350 $A^{-1/3}$ MeV in Heavy Nuclei

B. Bonin*, N. Alamanos*, B. Berthier*, G. Bruge*, J.L. Escudié*, H. Faraggi*, D. Legrand*, J.C. Lugol*, W. Mittig*, L. Papineau*, J. Arvieux**, L. Farvacque**, M. LeVine***, D.K. Scott, A.I. Yavin+ and M. Buenerd++

At present, most of the electric giant dipole resonances belonging to the 0, 1, 2 $\hbar\omega$ transitions are well established. They correspond to the isovector dipole and quadrupole modes and to the isoscalar quadrupole (GQR) and monopole (GMR) modes.[1] These resonances provide a unique source of information on the bulk properties of nuclei and nuclear matter, such as symmetry potentials, effective masses, and compressibility.[2] Interest is now moving towards the 3 and 4 $\hbar\omega$ resonances expected to lie at higher excitation energy. Recently, evidence has been found for the 3 $\hbar\omega$ octupole mode (HEOR).[3-5]

High resolution α-particle beams of energies above 50 MeV/nucleon provide a new experimental approach to the study of high energy multipole resonances. We report here evidence for isoscalar giant multipole strength up to 60 MeV of excitation energy (E*) in ^{208}Pb and ^{116}Sn and up to E* ≈ 45 MeV in ^{58}Ni, using inelastic scattering of α-particles at 340 and 480 MeV.

High velocity α-particle beams are interesting in several other respects: i) angular distributions display diffraction patterns obeying Blair phase rules; ii) small angle oscillations characterize the angular momentum transfer; iii) ^{5}He and ^{5}Li contributions are kinematically removed from the excitation region of interest; iv) the multiphonon contribution to background is expected to decrease because of the very short interaction time. However Coulomb excitation[6] may induce some contribution of isovector resonances mainly at small angles, but less than with T≠0 projectiles.

We have used α-particle beams of 340 and 480 MeV (85 and 120 MeV/nucleon respectively) from the Saturne synchrotron to bombard isotopically enriched ^{208}Pb, ^{116}Sn and ^{58}Ni targets. The scattered α-particles were analyzed by the SPES I magnetic spectrometer, with an energy resolution of about 300 keV. Particle identification was made by means of a dE/dX selection in the scintillator trigger. Inelastic scattering data were taken at 20 angles between 3 and 10 degrees. The excitation energy windows extended from 8 MeV to 38 MeV for the 480 MeV data, to 45 MeV for the 340 MeV data; moreover, ^{208}Pb at 340 MeV and ^{116}Sn at 480 MeV were investigated up to 60 MeV in excitation energy. An experimental spectrum for ^{208}Pb at 340 MeV incident energy is displayed in Fig. 1. Results on ^{116}Sn and ^{58}Ni are similar. A good separation of the GQR and GMR is observed and in addition, the spectrum shows that under the GQR-GMR peaks the

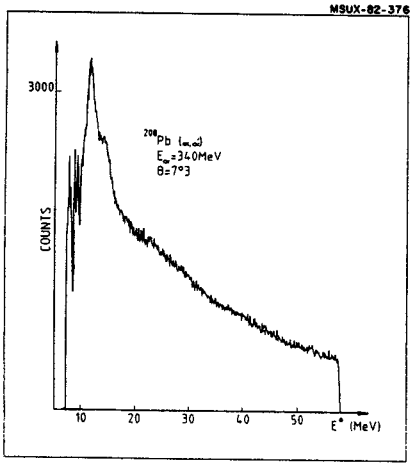

Fig. 1. Inelastic scattering spectrum for ^{208}Pb at an incident α energy of T_α = 340 MeV.

peak-to-background ratio is good, better than for lower energy experiments. Collective excitations around 115-120 $A^{-1/3}$ MeV are clearly visible. In addition, there is some indication for other groups at higher excitation energies.

Since angular distributions for the background are known to be monotonic, a three-dimensional representation of the experimental spectra (the horizontal coordinates of which are the scattering angle θ and the excitation energy E*) should show, above a gently varying surface, oscillations corresponding to giant resonances with well defined quantum numbers.

Fig. 2 shows such a matrix for ^{208}Pb at 480 MeV, in which two ranges A and B corresponding to the well known GQR and GMR resonances show up on the left hand side, with typical oscillations corresponding to even parity. The small vertical arrows under A and B indicate some fine structure in those groups. In addition, one may see dark horizontal bands parallel to the E* axis and denoted C, which appear to be oscillations out of phase with the GQR; they may therefore correspond to odd parity excitations. Some odd strength is spread over the experimental spectra from just above the GMR resonance, and extending beyond the previously known HEOR. Note that this characteristic is observed before any background subtraction. The same feature was found for ^{208}Pb at T_α=340 MeV, where the spectrum was investigated up to

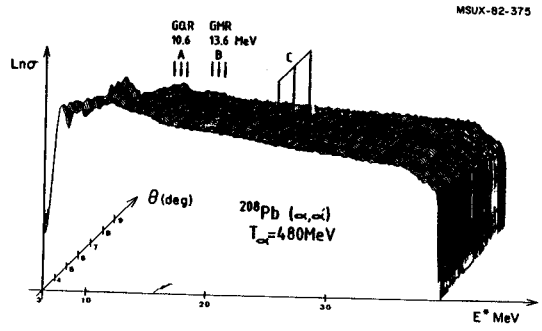

Fig. 2. Three dimensional plot of the spectra measured for ^{208}Pb at T_α = 480 MeV.

60 MeV in excitation energy. Two striking new facts show up: i) the odd parity oscillations are present all over the spectrum, i.e. up to E*=60 MeV; ii) beyond E*=35 MeV, there appear new intermediate lines which are typical of some even parity excitation. These data suggest the following qualitative interpretation: i) the $3\hbar\omega$ transitions, which include the HEOR, extend far beyond what is already known; ii) in addition, this structure begins at $E^* \cong 200\ A^{-1/3}$ MeV in ^{208}Pb. Both transitions (which should involve several multipolarities) extend up to the upper limit of our experimental spectra i.e. to $E^* \approx 350\ A^{-1/3}$ MeV in ^{208}Pb, in fair agreement with the RPA predictions of Gogny and Decharge[7] and the recent approach of Van Giai.[8]

After background subtraction, the resulting surface is projected into angular distributions corresponding to 1 MeV excitation energy bins. The analysis of the whole set of data is not completed yet, but all the angular distributions between 15 and 30 MeV in excitation energy (i.e. above the GQR-GMR region) are roughly in phase, and out of phase with the GMR angular distribution. There are noticeable changes in the slopes of the maxima and in the depths of the minima. As an example, three typical angular distributions are shown in Fig. 3 corresponding to $E^* \approx 19$, 24 and 29 MeV respectively. For comparison the solid line represents the experimental angular distribution for the first 3^- state at 2.61 MeV. As expected the HEOR appears to be the dominant contribution, however its strength seems to extend up to $E^* \cong 30$ MeV with a possible admixture of other multipolarities.

In conclusion, a three dimensional presentation of our data has enabled us to state that there is a good experimental evidence for odd giant multipole resonances extending up to quite

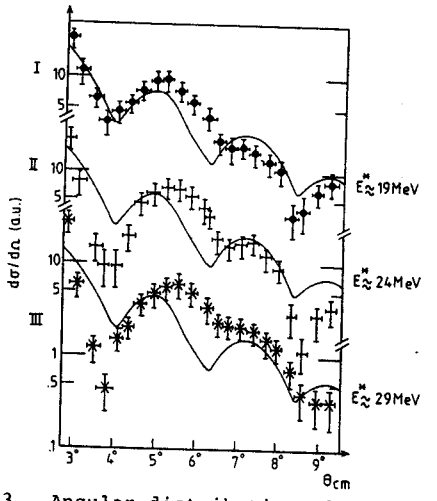

Fig. 3. Angular distributions for three 1 MeV wide energy bins centered at 19, 24 and 28 MeV in ^{208}Pb at T_α = 480 MeV. Drawn for comparison is a solid line corresponding to the experimental angular distribution measured for the first 3^- state at 2.61 MeV.

high excitation energies (60 MeV in ^{208}Pb) and that some even parity strength shows up above E* = 35 MeV in ^{208}Pb. A detailed reduction into the different multipolarities has to be done now in order to obtain from the data the full response function of ^{208}Pb, ^{116}Sn and ^{58}Ni for each dominant multipolarity. It will also be quite interesting to derive the empirical shape obtained here for the continuum from a more fundamental microscopic approach, calculating the different stages of multi-step direct-direct excitations, such as the one already used for the multi-step compound part.[9]

Our thanks are due to the Saturne technical staff for their efficient beam delivery. We also wish to thank the computer groups of the DPh-N/BE for valuable help in data processing. We are greatly indebted to D. Gogny, J. Decharge, R. Von Geramb and J. Raynal for enlightening discussions and for their predictive calculations.

* DPh-N, CEN Saclay, 91191 Gif-sur-Yvette, France.
** LNS, CEN Saclay, 91191 Gif-sur-Yvette, France.
*** DPh-N, on leave of absence from Brookhaven National Laboratory.
\+ DPh-N, on leave of absence from Tel-Aviv University, Israel.
++ ISN Grenoble, France.

1. F.E. Bertrand, Nucl. Phys. A354, 219 (1981).
2. J.P. Blaizot, Oak Ridge Conference 1979, ed. F. Bertrand, (Harwood Academic Press) p. 139.
3. T.A. Carey et al., Phys. Rev. Lett. 45, 239 (1980).

4. T. Yamayata et al., Phys. Rev. C23, 937 (1981).
5. H.P. Morsch et al., Phys. Rev. Lett. 45, 337 (1980).
6. M. Buenerd and D. Le Brun, Phys. Rev. C34, 337 (1981).
7. D. Gogny and J. Dechargé, Phys. Rev. C21, 1568 (1980) and private communication.
8. N. Van Giai, Phys. Lett. 105B, 11 (1981).
9. H. Feshbach et al, Ann. Phys. 125, 429 (1980).

Measurement of Beta Decay Halflives of Neutron-rich Nuclei

G.D. Westfall, L.H. Harwood, M.J. Murphy*, T.J.M. Symons*, and H.J. Crawford**

The study of the properties of neutron-rich nuclei far from the valley of stability provides valuable information basic to many problems in nuclear physics and astrophysics. The combination of measured masses and lifetimes allows the matrix elements of beta decay to be studied while beta decay lifetimes control the progress of stellar evolution and nucleosynthesis. The fragmentation of high energy heavy ions has proved to be a powerful method of producing neutron rich light nuclei with sixteen new nuclei being observed near the limit of stability.[1,2] This technique has been further extended to the measurement of beta decay halflives using the fragmentation of a 285 MeV/n ^{40}Ar beam where the previously unknown halflives of 220 and ^{32}Al were found to be 910+/-350 msec and 35+/-5 msec respectively.[3]

In this experiment, a 300 MeV/nucleon ^{56}Fe beam of approximately 107 particles/sec from the LBL Bevalac was fragmented using a 1 gram/cm^2 Be target. The neutron-rich projectile fragments passed through a zero-degree spectrometer with an angular acceptance of 1 msr. The fragments were stopped in an eight element silicon detector telescope located on the focal plane of the spectrometer. The telescope consisted of two 0.80 mm thick, 50 mm diameter trigger detectors and six 5 mm thick, 75 mm diameter position sensitive detectors as shown in Fig. 1. To suppress background, the telescope was surrounded with scintillators operated in an anticoincidence mode. A brass collimator was placed in front of the telescope to insure that no unwanted beta activities were deposited in the detector stack. A punch-through detector was placed behind the telescope to suppress energetic particles passing completely through the telescope.

The halflives of the neutron-rich fragments were measured by recording the time of arrival of the fragment, clamping the beam from the Bevalac, raising the gain of the preamplifiers by a factor of 100 to allow the detection of beta particles from the decay of the fragment, and then recording the energies and times of all beta decays until the next Bevatron beam pulse was ready (approximately 3 secs.). Background counts were suppressed by requiring that the beta decays originate from the detector in which the fragment stopped and that the position of the betas correlate with the position of the stopped fragment. Data analysis is in progress.

* Lawrence Berkeley Laboratory.
** University of California, Space Sciences Laboratory.

1. T.J.M. Symons, Y.P. Viyogi, G.D. Westfall, P. Doll, D.E. Greiner, H. Faraggi, P.J. Lindstrom, and D.K. Scott, Phys. Rev. Lett. 42, 40 (1979).
2. G.D. Westfall, T.J.M. Symons, D.E. Greiner, H.H. Heckman, P.J. Lindstrom, J. Mahoney, A.C. Shotter, D.K. Scott, H.J. Crawford, C. McParland, T.C. Awes, C.K. Gelbke, and J.M. Kidd, Phys. Rev. Lett. 43, 1859 (1979).
3. M.J. Murphy, T.J.M. Symons, G.D. Westfall, and H.J. Crawford, submitted to Phys. Rev. Lett. (1982).

MSUX-82-268

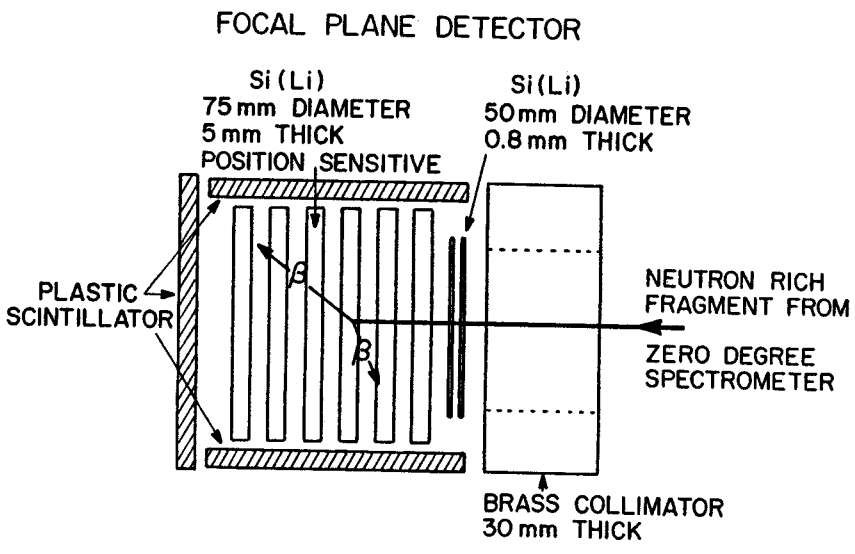

Fig. 1.

Gamow-Teller Strength at High Excitation

G. Bertsch and I. Hamamoto

The recent elucidation of the giant Gamow-Teller state in heavy nuclei by the (p,n) reaction presents a paradox. There is a well-defined peak whose energetics are reproduced by shell model theory,[1] but the strength is less than half the predicted value. We here calculate the amount of strength removed to high excitation energies. We study the nucleus ^{90}Zr, and use M3Y residual interaction[2] to calculate the interaction matrix elements between 2p-2h and simpler configurations. The single particle Hamiltonian is based on a Woods-Saxon potential, with the continuum discretized by requiring the wave functions to vanish at a radius of 12 fm.

The strength in the continuum is calculated in second-order perturbation theory, which can be expressed as the square of an amplitude containing the four graphs shown in Fig. 1. The

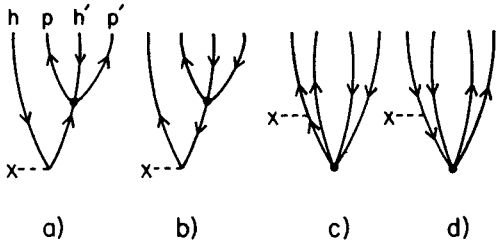

Fig. 1. Four types of amplitude included in the calculation.

first two graphs represent correlations of the particle or hole in an intermediate particle-hole state, and the last two graphs represent effects of ground state correlations. For the $\sigma\tau_-$ operator, these two processes are effectively incoherent. We find that particle correlations shift 38% of the total $\sigma\tau_-$ strength into the region of 10-45 MeV excitation, while ground state correlations give 20% in this region. The coherent total is 56%, which is an overesti-

The detailed strength distribution is shown in Fig. 2. We see some shell structure remaining at the lower excitations. This is an artifact of the 2p-2h approximation and is undoubtedly

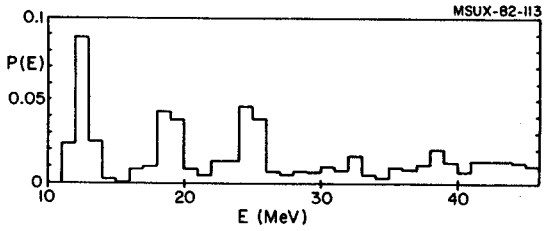

Fig. 2. Calculated strength distributed P(E) for the Gamow-Teller operator in ^{90}Zr. Energies are measured with respect to the ground state of ^{90}Nb, so that the unperturbed strength is at 0 and 6 MeV excitation. The normalization is $\int$ (P(E)dE=1, with E in MeV.

washed out by damping into more complex configurations. We also see that there is a smooth background of about 1%/MeV persisting up to quite high excitation. The amount of the strength is consistent with a continuum (p,n) cross section of 1 mb/sr due to the spreading of the Gamow-Teller strength.

In view of these large results, we intend to repeat the calculation under other conditions. First of all, it is necessary to carry the analysis to higher energies. It is not practical to extend our computation scheme directly, as the number of configurations increases very rapidly. In our present case we considered about 20,000 2p-2h configurations. However, we expect coherence between direct and exchange to be reduced at high energy. It should be feasible to calculate the incoherent sum to high enough energy to obtain the complete strength function. It will also be interesting to carry out this kind of analysis for other strength functions, for example the giant dipole and the giant quadrupole. In the case of the giant quadrupole, the coherence effects should rduce the strength at high excitation to a much smaller fraction of the total.

1. G. Bertsch, D. Cha, and H. Toki, Phys. Rev. C24, 533 (1981).
2. G. Bertsch, J. Borysowicz, H. McManus, and W. Love, Nucl. Phys. A284, 399 (1977).

Gamow-teller Strength in the (p,n) Continuum

O. Scholten, G.F. Bertsch and H. Toki

Recent high energy (p,n) experiments have provided systematic data on the Gamow-Teller (GT) strength in nuclei. There is a well-defined GT peak, but it has less than 50% of the expected strength, based on an analysis utilizing the known GT ft-values and the Gamow Teller sum rule

$$S(\beta^- - \beta^+) = \sum_n (\langle n \mid t_- \mid 0 \rangle^2 - \langle n \mid t_+ \mid 0 \rangle^2) = 3(N-Z)$$

There are several mechanisms proposed to explain the missing GT strength. We want to see if part of the strength is in the continuum background at high excitation energies. In this respect, an interesting observation can be made on the 0^o spectra of several nuclei presented in Fig. 5 or Ref. 1. The area of the long tail (continuum) seems to be proportional to the peak area. This observation may imply that a large portion of the background cross section is due to the Gamow-Teller strength brought up from the low energy region. Therefore, we try to extract the GT strength in the continuum using the DWBA angular distributions for individual angular momentum transfers.

The optical model parameters were taken from Ref. 2 and we used macroscopic form factors. DWBA calculations reproduce angular distributions for discrete states quite well. Because only L=0 angular distribution peaks at 0^o the unfolding procedure works reasonably well for assigning the L=0 strength. We present a result of such a decomposition procedure into several L's at E_x=30 MeV of the 200 MeV ^{90}Zr (p,n) spectrum in Fig. 1. This procedure works very well at all angles. In this analysis, we used the result of the semi-infinite slab quasi-elastic model[3] to account for the single particle knock-out process which provides the gross feature of the continuum. We found about 40% of the cross section is due to L=0. A similar analysis without the use of the quasi-elastic result gave essentially the same strength for L=0.

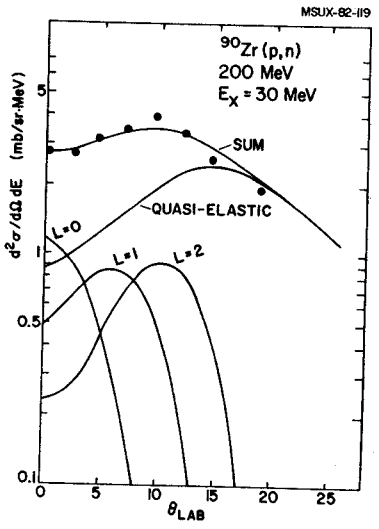

Fig. 1. Decomposition of the angular distribution into several angular momentum transfers observed in the 200 MeV (p,n) reaction on ^{90}Zr at E_x=30 MeV in excess of the quasi-elastic background as calculated in Ref. 3.

We further performed the decomposition up to E_x=45 MeV, but the analysis became difficult above $E_x \gtrsim 50$ MeV because the L=1 angular distribution becomes forward peaked also due to large momentum transfer associated with high energy transfer even at $\theta = 0^o$. The extracted L=0 strength would correspond to the cross section of 2 mb/sr MeV at $\theta = 0^o$ at the energy loss of the Gamow-Teller resonance. If we assume the same strength over the energy interval between 15 and 45 MeV as supported by our analysis, we could account for more than half of the missing GT strength.

This finding agrees with the result of the recent 2p-2h response function calculation of Hamamoto and Bertsch.[4] It is very important to extend this kind of analysis to other cases, in order to understand the problem of the missing Gamow-teller strength.

1. C. Gaarde et al., Nucl. Phys. 369, 258 (1981).
2. J.M. Moss et al., Phys. Rev. Lett. 48, 789 (1982).
3. G.F. Bertsch and O. Scholten, Phys. Rev. C25, 804 (1982).
4. G.F. Bertsch and I. Hamamoto, to be published in Phys. Rev. C26, (1982).

The $\sigma\tau_+$ Strength in Nuclei

D. Cha and G.F. Bertsch

In recent studies,[1] it has been found that the $\sigma\tau_-$ and the $\sigma\tau_z$ resonances observed by intermediate energy protons show significant reduction in strength compared to the shell model estimations. Here, we study the $\sigma\tau_+$ strength with a zero range interaction. Although the same reaction mechanism governs all three modes, its structure may be quite different due to the asymmetry between protons and neutrons in the parent nucleus.

The theory is the quasi-particle random phase approximation. The initial state is approximated by the BCS ground state from a Woods-Saxon potential with pairing correlations between like nucleons only. As for the strength of the particle-hole interaction, it is determined from the main peak of the $\sigma\tau_-$ strength.[2] The strength of the particle-particle interaction is deduced from the lowest 1^+ state in ^{42}Sc which can be regarded as a pure particle-particle state above the doubly magic ground state of ^{40}Ca.

In Fig. 1, the results are compared with the log(ft) values of the β^+ decay of even-even neutron rich nuclei between mass numbers A=100~150. With no residual interaction, the pairing correlation alone predicts about 30 to 40 times more strength than what has been observed. The ground state correlation then reduces the strength by a factor of about 10. In general, we find the data are overestimated by the theory by about three to ten times (0.5 ~ 1.0 difference in log(ft) values). This confirms the findings in other modes which show quenching by about three. This extra reduction in strength must be found somewhere else outside the present model space, for example from the collective Δ-hole excitation,[3] or from more complex configurations.[4]

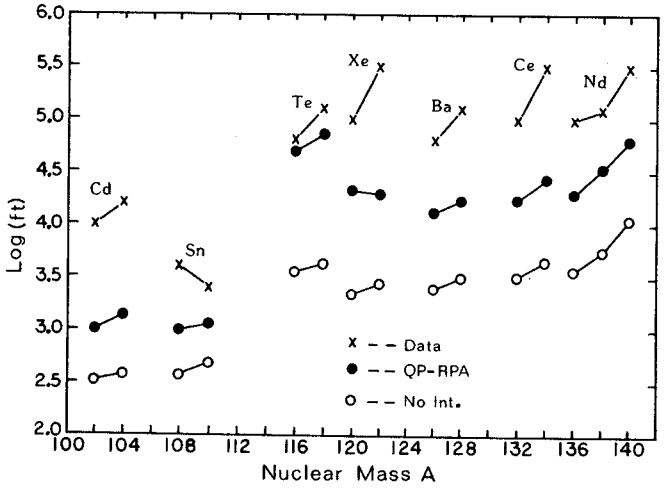

Fig. 1. Log(ft) values of the β^+ decay of even-even nuclei between A=100 ~ 150.

We also find from Fig. 1 that the data and the theory altogether is divided into two groups: one group including cadmium and tin isotopes and the other group with all other nuclei. The strength of the first group is around one order of magnitude larger than that of the second group. This is the result of the ground state configuration of protons in the parent nucleus. The first group has protons up to the Z=50 major shell while the second group has protons above it. Since the transition amplitude is larger for a larger j and $g^{\pi}_{9/2}$ is the highest proton j-orbit, two-quasi-particle state $g^{\pi}_{9/2}g^{\nu}_{7/2}$ is the most dominant unperturbed state for all the nuclei we have treated. It happens to be the lowest unperturbed state for the first group as shown in Fig. 2a. When protons start to occupy levels above the major shell, there appears another significant two-quasi-particle state, $d^{\pi}_{5/2}d^{\nu}_{5/2}$, which is lower in energy than $g^{\pi}_{9/2}g^{\nu}_{7/2}$ as shown in Fig. 2b. Because of this, there is large reduction of the β^+ decay strength for nuclei above the tin isotope. For this group of nuclei, our theory predicts large concentration of the strength right above the Q window as shown in Fig. 2b. This resonance may be found by future experiments such as the (n,p) reaction. In fact, some evidence of this sort has been already observed in the β^+ decay of the odd mass nuclei. This is possible because the β decay Q values of the odd mass nuclei are about twice as large as those of the even mass nuclei. One example is the β^+ decay of ^{145}Gd measured recently by Firestone et al.[5]

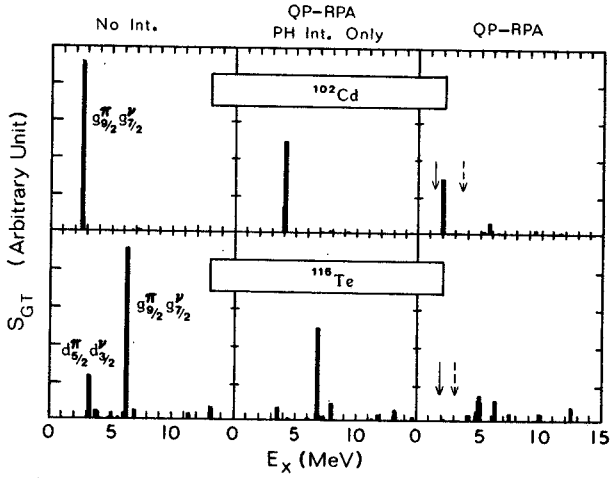

Fig. 2. The $\sigma\tau_+$ strength distribution of (a) ^{102}Cd and (b) ^{116}Te. The ground state (solid) arrow) of the daughter nucleus and the Q-window (dotted arrow) are deduced from comparing the theory and the data.

1. N. Anantaraman et al., Proc. Indo-U.S. Joint Symposium on "Nuclear Physics at Cyclotron and Intermediate Energies" (Bombay, India, 1982); S. Sagawa and N.V. Giai, Phys. Lett. 113B (1982) 119.
2. G. Bertsch et al., Phys. Rev. C24 (1981) 533.
3. A. Bohr and B.R. Mottelson, Phys. Lett. 100B (1981) 10; G.E. Brown and M. Rho, Nucl. Phys. A372 (1981) 397.
4. G. Bertsch and I. Hamamoto, Phys. Rev. C26 (1982) 1323.
5. R.B. Firestone et al., Phys. Rev. C25 (1982) 527.

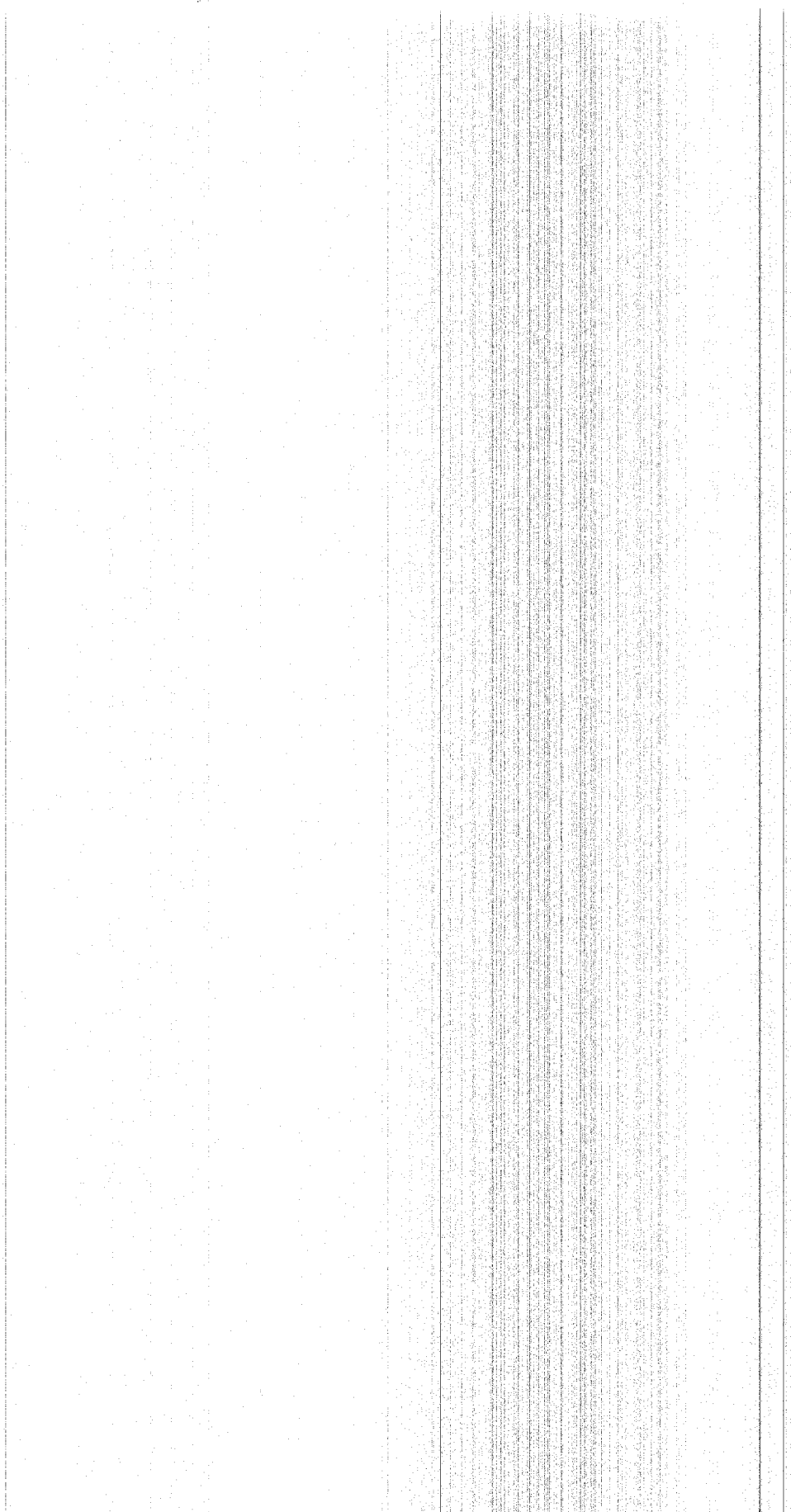

Isospin Dependence of Pion Absorption by a Nucleon Pair in He Isotopes

H. Toki and H. Sarafian

Recently, Ashery et al.[1] performed correlation measurements on outgoing nucleons after pion absorption at the kinetic energy of T =165 MeV in ^{3}He and ^{4}He. They found a surprisingly large ratio between the absorption cross sections by T=0 and T=1 initial nucleon pairs, on the order of $R=d\sigma(T=0)/d\sigma(T=1) \sim 50$. The isospin consideration alone results in R=2.

In order to understand the origin of this large ratio, we took the P-wave pion absorption model through Δ isobars (Fig. 1). This model has been demonstrated to explain the pionic disintegration of a deuteron in great detail[2] and also to provide microscopic understanding of π-nucleus optical potential parameters.[3]

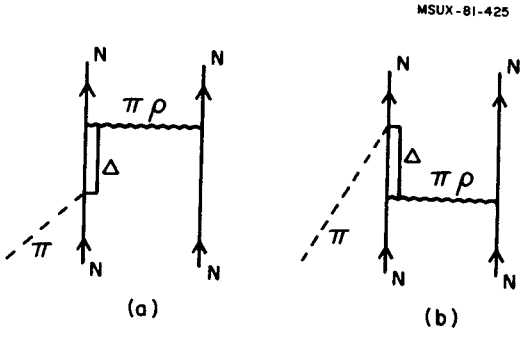

Fig. 1. p-wave pion absorption mechansim with Δ isobar intermediate excitation. (a) direct graph. (b) crossed graph.

We obtain an expression for the pion absorption two-body operator in momentum as well as in coordinate space with only the nucleon space operators.[4] The calculated results on the cross sections for several pion partial waves ($\ell_\pi \leq 2$) with T=0 and T=1 initial nucleon pairs are compared in Table I. The cross sections for ℓ_π=3 are further reduced by an order of magnitude.

Table I. Pion absorption cross sections in several channels as a function of pion momentum k are compared, where ℓ_π is the angular momentum of the incoming pion. These numbers are normalized to the (T,S,L)=(0,1,0) to (T',S',L')=(1,0,2) transition at k=0.5μ as indicated by *.

k[u]					0.5	1.0	1.5	2.0	2.5
Initial	ℓ_π	T'	S'	L'					
T=0	0	1	1	1	0.027	0.40	2.9	9.7	7.3
S=1	1	1	0	2	1*	4.9	21	52	30
L=0	2	1	1*	3	0.006	0.11	1.0	4.2	3.6
T=1	0	1	1	1	0.008	0.086	0.44	1.1	0.63
S=0	1	0	1	2	0.076	0.17	0.24	0.26	0.26
L=0	2	1	1	3	0.002	0.023	0.14	0.40	0.26

ℓ_π=1 pion absorption by a T=0 pair is by far dominant. The reasons are (i) ℓ_π=1 absorption by a T=1 pair in the direct process (Fig. 1(a) is forbidden by the Pauli principle and it is possible only in the crossed channel (Fig. 1(b) (ii) $\ell_\pi \neq 1$ abosrption by a 1S-orbit nucleon forces a Δ isobar to be excited in an orbit $\ell \leq 1$. This fact together with the short range nature of the process makes the spatial matrix elements for $\ell_\pi \neq 1$ typically one-fifth of that for ℓ_π=1.

The summed values for each T spin are then used to obtain the ratio R as a function of the pion momentum k (pion energy T). The dotted line in Fig. 2 is the result with ℓ_π=1 alone, while the solid line includes all the partial waves. The ratio at T_π=165 MeV comes out to be about 30, which is to be compared with the experimental results depicted by the dots with error bars taken at two different angles. The P-wave rescattering mechanism through nucleon intermediate excitations may give additional contribution to the T=1 cross section. The S-wave rescattering mechanism is known to be only significant below T ≲ 50 MeV.

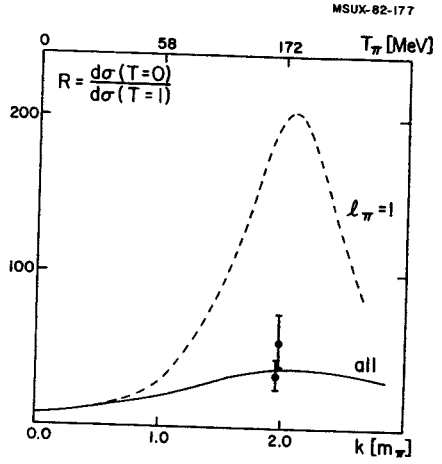

Fig. 2. The pion absorption ratio $R=d\sigma(T=0)/d\sigma(T=1)$ as a function of incoming pion momentum k in pion mass unit. The dashed line denotes the result with ℓ_π=1 only and the solid line that with all partial waves. Experimental data obtained at two different angles are also shown at $k=2m_\pi$ (T_π =165 MeV) with error bars.

1. D. Ashery et al., Phys. Rev. Lett. 47, 895 (1981).
2. O.V. Maxwell, W. Weise and M. Brack, Nucl. Phys. A348, 388 (1980).
3. J. Chai and D.O. Riska, Nucl. Phys. A329, 429 (1979).
4. H. Toki and H. Sarafian, to be published in Phys. Lett. B.

Two Δ Isobar Mechanism for Pion Absorption in Heavy Nuclei

G.E. Brown, W. Weise and A. Wirzba Stony Brook

H. Toki, NSCL

Recent measurements of the inclusive (π,p) reaction at energies T ~ 180 MeV suggest that pion absorption takes place on several nucleons (about 4).[1] This suggestion was made due to the experimental finding that the angular distribution is isotropic in a moving frame, the velocity of which gives the number of participating nucleons for pion absorption, and an expected peak due to the two nucleon mechanism at half the incoming pion energy is hardly seen.[1] Furthermore, several arguments were made against the picture where the final state interaction between the primary nucleons, produced by the two nucleon absorption mechanism, and other nucleons leads to emission of more than two low energy nucleons.

Motivated by this observation, we set up a model where two Δ isobars are formed instead of the decay into two nucleons after pion absorption; and each of them interacts with another nucleon to result in four nucleons.[2] The pion decay for the Δ isobars is largely prohibited by the phase space, since the intermediate isobars carry about half of the incoming pion energy ($\sim m_\pi$).

We argue this mechanism to be responsible for pion absorption in heavy nuclei by comparing the absorption cross section to that of the two nucleon mechanism. The important results obtained by working through the spin-isospin matrix elements are that an initial nucleon pair which turns into 2Δ after pion absorption in the 2Δ mechansim should have S=1 and T=1 and therefore L=odd, whereas a pair for the 2N mechanism should have S=1, T=0, and L=0. Hence, the number of nucleon pairs in the 2Δ process is much larger than that of the 2N process. In nuclei as heavy as ^{208}Pb, our estimate shows that the 2 process wins by a factor 5 ~ 10 over the 2N process. This 2Δ mechanism for pion absorption is able to reproduce the experimental data on the ratio of the yields of protons after π^+ and π^- absorption.

This 2Δ mechanism should have large impact on the double charge exchange reaction (π^+,π^-) around the resonance energy and the pion production at large incoming pion energy.

1. R.D. McKeown et al., Phys. Rev. Lett. 44, 1033 (1980).
2. G.E. Brown, et al., Phys. Lett. 118B (1982)39.

Microscopic Calculation of the Operators in the Interacting Boson-Fermion Model

O. Scholten and S. Pittel*

The interacting Boson-Fermion Model[1] (IBFM) can be regarded as an approximation to the nuclear shell model for the description of Odd-A nuclei. In the IBFM the basis states are built up out of s- and d-boson creation operators and a single fermion creation operator. The s and d bosons correspond[2] to the fermion operators s^+ and D^+ that create a collective fermion pair state with L=0 and 2,

$$S^+ = \sum_j \alpha_j \hat{j} (c_j^+ c_j^+)^{(0)} \qquad (1)$$

and

$$D^+ = \sum_{j_1 \leq j_2} \beta_{j_1 j_2} \frac{1}{\sqrt{1+\delta_{j_1 j_2}}} (c_{j_1}^+ c_{j_2}^+)^{(2)}. \qquad (2)$$

To establish a correspondence between states in the IBFM and the shell model space, the (S,D) states in the latter have to be projected on generalized seniority[3] (V) to create an orthogonal set of states. Operators are mapped from the shell-model space onto the IBFM space by equating matrix elements between corresponding states. For this purpose the matrix elements of operators between states with $v \leq 3$ are necessary. Recently we have developed analytix formulas to calculate these matrix elements.

Approximate expressions for the IBFM and IBM[4] operators can be obtained by introducing the pseudo-single particle (psp) operators,[5] which are the IBFM equivalent of the shell-model single particle operators, but take into account the fermion structure of the bosons. In Ref. 4 a simple formula for the pseudo-single particle operators is derived, partially based on the Number Operator Approximation.[2] This approximation is based on the assumption that the coefficients in Eq. (1) are all about equal. The matrix elements of the pseudo particle operator have been compared with those obtained from an exact calculation in the fermion space using our analytic formulas. In this calculation we have choices for α values which are appropriate for the 50-82 shell, $\alpha_{g_{7/2}}=0.9$, $\alpha_{d_{5/2}}=0.8$, $\alpha_{h_{11/2}}=0.3$, $\alpha_{d_{3/2}}=0.1$, and $\alpha_{s_{1/2}}=0.05$. Although these values are vastly different, the matrix elements calculated with the approximate formula[5] in the IBFM space agree to within 20% with the exact results for the lowest seniority states.

The pseudo particle operators can also be used to calculate the IBFM and IBM images of other operators such as the quadrupole operator.[5] Also in this case a good agreement between the exact and approximate results is found.

---

* Bartol Research Foundation

1. F. Iachello and O. Scholten, Phys. Rev. Lett. 43, 679 (1979).
2. T. Otsuka, A. Arima and F. Iachello, Nucl. Phys. A309, 1 (1978).
3. I. Talmi, Nucl. Phys. A172, 1 (1971).
4. A. Arima and F. Iachello, Ann. Phys. (N.Y.) 99, 253 (1976); 111, 201 (1978); 123, 468 (1979).
5. O. Scholten, Ph.D. Thesis, University of Groningen (1980); O. Scholten and A.E.L. Dieperink, in Interacting Bose-Fermi Systems in Nuclei, ed. F. Iachello (Plenum, New York, (1981) p. 343.

Shell Model Calculations for the N=82 Isotones

H. Kruse and B.H. Wildenthal

The N=82 isotones have recently received renewed attention due to the suggested sub-shell closure at ^{146}Gd (N=82, Z=64). We have performed shell model calculations for the N=82 nuclei from Z=52 to Z=66. The model space consists of five orbits, namely $0g_{7/2}$, $1d_{5/2}$, $1d_{3/2}$, $2s_{1/2}$ and $0h_{11/2}$. Without some truncation scheme the resulting dimensions would exceed even the capabilities of present-day computers. We therefore restrict our model basis to wave functions with seniority less than or equal to 4. In addition we require that the occupation of the $0h_{11/2}$ orbit not exceed four particles.

This model space has been used for the entire chain of nuclei considered. We have derived a single, empirical Hamiltonian for the entire chain by adjusting single-particle energies and two-body matrix elements to obtain an optimal agreement with the experimentally known levels.

The energy spectra computed in this way agree well with the observed ones up to excitation energies of about 2 MeV for odd-mass systems, and about 3 MeV for even-mass nuclei. High-spin states at higher excitation energies are also well reproduced. The only systematic discrepancy between the observed and the computed spectra involves the lowest measured 3^- levels. These levels are consistently predicted at excitation energies of about 1 MeV above the observed values. It seems clear that the wave functions for these levels must contain large components from outside of our model space.

In Fig. 1 we show a comparison of computed and experimental spectra for ^{144}Sm, ^{146}Gd, and ^{148}Dy. With the exception of the 3^- levels mentioned above, the agreement between calculated and observed levels is consistently good; in particular all features which lead to the assumption of a shell closure in ^{146}Gd are well reproduced. On examination of the wave functions for ^{146}Gd one finds, however, that the ground state as well as the excited states contain a larger than 50% admixture of $(0g_{7/2}, 1d_{5/2})^{-n}\ 0h_{11/2}{}^{n}$ hole-particle excitations.

This result clearly illustrates the elusive nature of a shell closure. The structure of the wave functions is continuous across the "closure", contrary to the break suggested by examining the experimentally observable data.

We are currently completing the task of refining the model Hamiltonian and will then begin to study transition rates and spectroscopic factors.

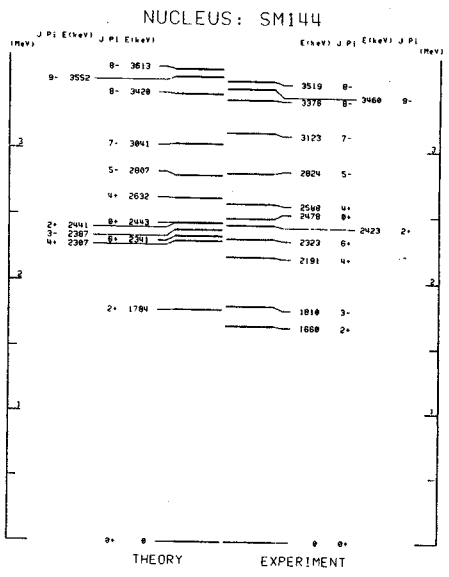

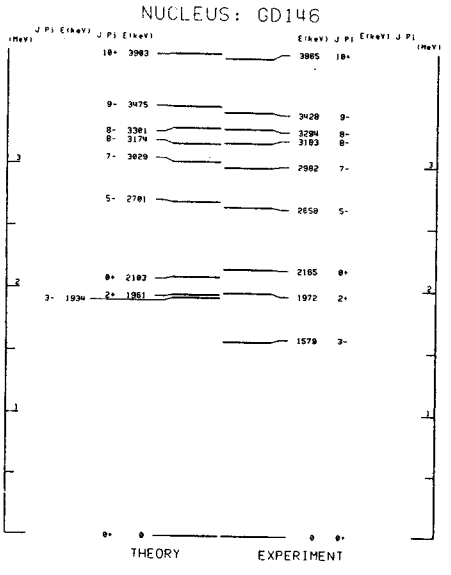

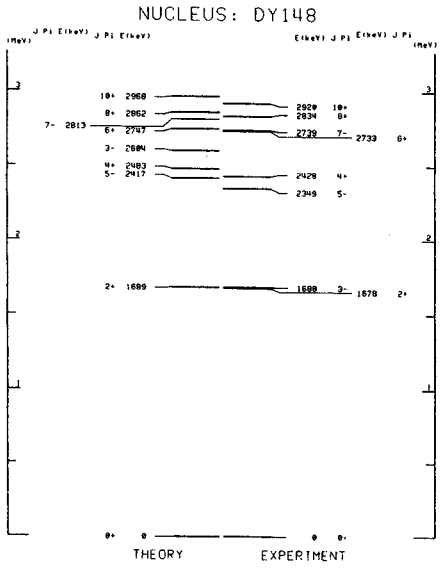

Fig. 1(a) - (c): A comparison of computed and measured excitation energies in ^{144}Sm, ^{146}Gd, and ^{148}Dy. Only those theoretical levels which have an experimental counterpart, are shown. Note that different energy scales are used in the three figures.

The Formulation of an Empirical Hamiltonian Suitable for Calculations throughout the 0d,1s Shell

B.H. Wildenthal

A set of single-particle energies and two-body matrix elements of a "$0d_{5/2}$-$1s_{1/2}$-$0d_{3/2}$" shell-model Hamiltonian, designed for use in the complete sd vector space, has been obtained from a fit to 440 experimental energies of levels occurring in nuclei of all A values from 17 through 39. This empirical Hamiltonian yields a good accounting of the energy spectra of intra-sd-shell states throughout the region. The essential feature to achieving this comprehensive reproduction of experimental spectra from a single formulation of the Hamiltonian is the incorporation into the two-body matrix elements of a dependence upon the mass number A. This was done by multiplying the two-body matrix elements values of the Hamiltonian to be used for levels in A-nucleon nuclei by a common factor of $(18/A)^{0.3}$. The single-particle energies are the same for all values of A.

While an accurate, realistic treatment of the A (or size) dependence of the Hamiltonian matrix elements is obviously more complex than our simple scaling, the dominant trend in, for example, Kuo's two-body matrix elements for the sd-shell, is consistent with our assumption. In any case, some average reduction in magnitude of the two-body matrix elements as A increases is obviously more physically realistic than an absolute invariance. The precise power of A is not, as far as we have determined, critical nor is its optimum value well defined. Possible choices seemed to range between 0.2 and 0.4.

Some of the improvements over the A-invariant formulations of Preedom-Wildenthal and Chung-Wildenthal which the new Hamiltonian embodies are self-evident. We mention in particular the intrinsically better treatment which the new formulation should yield for the nuclei in the A = 25-31 region, especially those with large assymetries in their neutron and proton numbers. Beyond this sort of issue, moreover, the new energies and wave functions throughout the A=20-36 range appear, upon initial inspections, to be on the average superior to the older results. As an example of the results obtained with this new Hamiltonian, we compare in Figure 1 predicted neutron separation energies with experimental values.

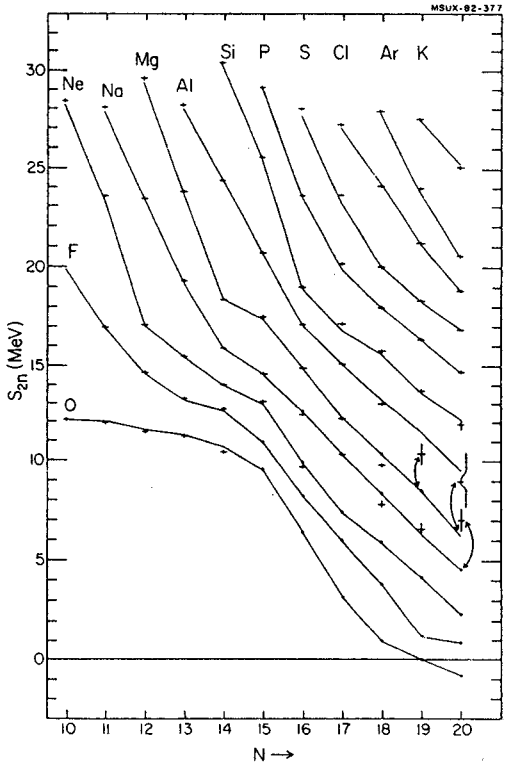

Fig. 1.

Longitudinal E2 and E4 Form Factors for Inelastic Electron Scattering on Doubly-Even sd Shell Nuclei

B.A. Brown, R. Radhi and B.H. Wildenthal

We have studied the relationships of shell-model-based theoretical form factors for E2 and E4 inelastic electron scattering on doubly-even sd-shell targets to the existing body of experimental data. The shell-model wave functions utilize the complete $0d_{5/2}$-$1s_{1/2}$-$0d_{3/2}$ basis spaces for A-16 nucleons and are obtained by diagonalizations of a new empirical Hamiltonian designed for universal use in the A = 18-38 region. We have investigated in detail the effects upon the final results of the various auxiliary theoretical inputs which are necessary in order to translate the shell-model one-body transition density matrix elements into (e,e') form factors. We have compared the predictions obtained with the plane-wave Born approximation for the (e,e') reaction with those obtained in the distorted-waves approximation. The effects of choosing single-particle wave functions derived from, alternatively, harmonic oscillator, energy-dependent and independent Saxon-Woods, and self-consistent Skyrme-type potentials are documented. Theory and experimental data for elastic scattering from the ground states are studied to establish their consistency with the inelastic scattering process to the 2^+ and 4^+ states.

Finally, the effects of how the "effective charges" are entered into the theory are studied by comparing results obtained by assuming an effective-charge density with results obtained by assuming a Tassie model shape for the effective-charge transition density. The consistency of the (e,e') results with B(E2) measurements at the photon point is studied in the individual cases and overall via comparison of the data to form factor normalizations set by the effective charge normalizations $\delta e_p = \delta e_n = 0.35e$ for E2 and $\delta e_p = \delta e_n = 0.5e$ for E4.